Systematic mapping of chemoreceptor specificities for *Pseudomonas aeruginosa*

Wenhao Xu[a], Jean Paul Cerna-Vargas[b,c], Ana Tajuelo[b*], Andrea Lozano Montoya[b], Melissa Kivoloka[a], Nicolas Krink[a*], Elizabet Monteagudo-Cascales[b], Miguel A. Matilla[b], Tino Krell[b#], Victor Sourjik[a#]

[a]Max Planck Institute for Terrestrial Microbiology & Center for Synthetic Microbiology (SYNMIKRO), Marburg, Germany

[b]Department of Biotechnology and Environmental Protection, Estación Experimental del Zaidín, Consejo Superior de Investigaciones Científicas, Granada, Spain

[c]Centro de Biotecnología y Genómica de Plantas CBGP, Universidad Politécnica de Madrid-Instituto Nacional de Investigación y Tecnología Agraria y Alimentaria/CSIC, Parque Científico y Tecnológico de la UPM, Pozuelo de Alarcón, Madrid, Spain

[*]Present address: Intrahospital Infections Laboratory, National Centre for Microbiology, Instituto de Salud Carlos III (ISCIII), Madrid, Spain (Ana Tajuelo); The Novo Nordisk Center for Biostability, Danish Technical University, Kgs Lyngby, Denmark (Nicolas Krink)

#Address correspondence to Tino Krell, tino.krell@eez.csic.es, or Victor Sourjik, victor.sourjik@mpi-marburg.mpg.de

Running Head:

Ligand mapping for *P. aeruginosa* chemoreceptors

Abstract

The chemotaxis network, one of the most prominent prokaryotic sensory systems, is present in most motile bacteria and archaea. Although the conserved signaling core of the network is well characterized, ligand specificities of a large majority of diverse chemoreceptors encoded in bacterial genomes remain unknown. Here we performed a systematic identification and characterization of new chemoeffectors for the opportunistic pathogen *Pseudomonas aeruginosa*, which has 26 chemoreceptors possessing most of the common types of ligand binding domains. By performing capillary chemotaxis assays for a library of growth-promoting compounds, we first identified a number of novel chemoattractants of varying strength. We subsequently mapped specificities of these ligands by performing Förster resonance energy transfer (FRET) and microfluidic measurements for hybrids containing ligand binding domains of *P. aeruginosa* chemoreceptors and the signaling domain of the *Escherichia coli* Tar receptor. Direct binding of ligands to chemoreceptors was further confirmed *in vitro* using thermal shift assay and microcalorimetry. Altogether, the combination of methods enabled us to assign several new attractants, including methyl 4-aminobutyrate, 5-aminovalerate, L-ornithine, 2-phenylethylamine and tyramine, to previously characterized chemoreceptors and to annotate a novel purine-specific receptor PctP. Our screening strategy could be applied for the systematic characterization of unknown sensory domains in a wide range of bacterial species.

Importance

Chemotaxis of motile bacteria has multiple physiological functions. It enables bacteria to locate optimal ecological niches, mediates collective behaviors, and can play an important role in infection. These multiple functions largely depend on ligand specificities of chemoreceptors, and

the number and identities of chemoreceptors show high diversity between organisms. Similar diversity is observed for the spectra of chemoeffectors, which include not only chemicals of high metabolic value but also bacterial, plant and animal signaling molecules. However, the systematic identification of chemoeffectors and their mapping to specific chemoreceptors remains a challenge. Here, we combined several *in vivo* and *in vitro* approaches to establish a systematic screening strategy for the identification of receptor ligands, and we applied it to identify a number of new physiologically relevant chemoeffectors for the important opportunistic human pathogen *P. aeruginosa*. This strategy can be equally applicable to map specificities of sensory domains from a wide variety of receptor types and bacteria.

Keywords: *Pseudomonas aeruginosa*, chemotaxis, signal transduction, ligand binding domains, chemoeffectors, receptor chimera, Förster resonance energy transfer (FRET), purines, amino acids, biogenic amines

Introduction

Most bacteria have evolved the ability to detect a wide range of environmental signals to survive and grow under rapidly changing conditions. One of the most prominent prokaryotic sensory systems is the chemotaxis network that controls motility (1, 2). Chemotaxis has multiple important functions in bacterial physiology, dependent on the lifestyle and ecological niche, enabling bacteria to move towards optimal growth environments but also mediating collective behaviors and interactions with eukaryotic hosts (3, 4).

Such variety of chemotaxis-mediated functions is primarily ensured by the diversity of bacterial chemoreceptors, also called methyl-accepting chemotaxis proteins (MCPs) (5). While the core of the signaling pathway is conserved among bacteria, the number and specificity of chemoreceptors is highly variable and strain-specific (6). The reported repertoire of signals recognized by chemoreceptors across bacterial species includes proteinogenic amino acids (7, 8), polyamines (9), quaternary amines (10), nucleobases and their derivatives (11, 12), organic acids (13, 14), sugars (15), but also inorganic ions (16, 17), pH (18–20) and temperature (21, 22). Nevertheless, the signal specificity remains unknown for the absolute majority of chemoreceptors.

The paradigmatic model system of *Escherichia coli* chemotaxis consists of a single pathway, controlled by four transmembrane chemoreceptors and one aerotaxis receptor, and it includes six cytoplasmic signaling proteins: a histidine kinase CheA, an adaptor CheW, a response regulator CheY, a methyltransferase CheR, a methylesterase CheB, and a phosphatase CheZ (2). Typically, chemotactic stimuli modulate the autophosphorylation activity of CheA, which is inhibited by attractants and stimulated by repellents, subsequently altering the transphosphorylation of CheY. The phosphorylated CheY binds to the flagellar motor resulting in a change in the direction of flagellar rotation, ultimately causing a chemotactic response. CheZ is responsible for the dephosphorylation of CheY. After the initial pathway response, an adaptation system composed of CheR and CheB adjusts the level of receptor methylation on several specific glutamyl residues, providing negative feedback to the kinase activity, which ensures adaptation of cells to persisting stimulation. Although most of the chemotaxis proteins found in *E. coli* are conserved across bacterial chemotaxis pathways, most bacteria have more complex chemosensory pathways,

possessing additional chemotaxis proteins and chemoreceptors, alternative adaptation and signal termination strategies (23–25).

Canonical chemoreceptors can be separated in three functional domains: a periplasmic ligand binding domain (LBD), a signal conversion HAMP domain, and a cytoplasmic signaling domain that interacts with the autokinase CheA (5). Analyses of sequenced bacterial genomes revealed that bacterial chemoreceptors employ more than 80 different types of LBDs (6). In contrast, all *E. coli* transmembrane chemoreceptors possess the same four-helix bundle (4HB) type of LBD. Thus, although *E. coli* chemotaxis signaling pathway is one of the simplest and best understood, it does not represent the diversity of bacterial sensory capabilities.

Pseudomonas aeruginosa is among the most important human pathogens, causing the death of more than half a million people annually (26), and it is also one of the most well-studied alternative models for chemotaxis (27, 28). The chemoreceptor repertoire of the *P. aeruginosa* model strain PAO1 has 26 chemoreceptors containing 12 different LBD types that feed into four different chemosensory pathways, of which 23 chemoreceptors were predicted to stimulate the genuine F6-type chemotaxis pathway that controls swimming motility. Other three receptors McpB/Aer2, WspA, and PilJ are involved in an F7-type pathway of unknown function, an alternative cellular function pathway that mediates c-di-GMP synthesis, and type IV pili chemosensory pathway that is associated with twitching motility, respectively. The latter two pathways were found to perform mechano- and surface sensing rather than chemosensing (29–31). Of the 18 chemoreceptors with a periplasmic LBD that belong to the F6 pathway (28), ten have been functionality annotated (Table 1). Ligands of the other eight chemoreceptors involved in chemotactic behaviors are yet to be characterized, and given the variety of ligands that are

112 typically sensed by a single LBD, even the annotated LBDs are likely to possess additional ligand
113 specificities.

114 Several experimental approaches have been developed to systematically characterize the
115 specificities of uncharacterized chemoreceptors. The quantitative capillary chemotaxis assay is a
116 traditional method for identifying bacterial chemoeffectors. However, because of differences in
117 motility and physiology, the experimental conditions for the capillary assay need to be
118 established for each individual bacterial strain, which complicates its general application.
119 Moreover, assignment of identified ligands to specific chemoreceptors typically requires the
120 construction of strains with deletions of individual receptor genes, and it is complicated by the
121 frequent functional redundancy of multiple chemoreceptors. Alternatively, biochemical assays
122 can be used for ligand identification *in vitro* (32). The thermal shift assay (TSA; alternatively
123 called differential scanning fluorimetry, DSF) can be applied to characterize binding of chemical
124 compounds to LBDs in high-throughput screens, but it is prone to yield false-positive results.
125 Isothermal titration calorimetry (ITC) is, in contrast, an accurate but low-throughput method to
126 measure ligand binding (33). Although a combination of these *in vitro* methods has proven to be
127 very powerful for ligand identification (34), their application is limited to the LBD that can be
128 purified and to compounds with high-affinity binding.
129
130 A complementary strategy for identification of receptor ligands relies on the construction of
131 chimeric receptors that combine an LBD of interest with the well-characterized output domain,
132 such as that of the *E. coli* Tar receptor. Both, chemoreceptor-chemoreceptor hybrids (35) and
133 chemoreceptor-histidine kinase hybrids (36) that enable an *in vivo* readout of signaling response
134 have been recently used to annotate unknown sensory functions. Here, we constructed a library of

most *P. aeruginosa* LBDs fused to the signaling domain of the *E. coli* chemoreceptor Tar, and we used this library in combination with *in vivo* and *in vitro* assays to identify several novel physiologically relevant chemoeffectors and to assign them to specific *P. aeruginosa* chemoreceptors. Overall, our screening strategy allowed us to expand the list of known chemoreceptor specificities for *P. aeruginosa*, and a similar approach should be applicable to chemoreceptors from other bacteria and even to other types of receptors with a periplasmic LBD.

Results

High-throughput screening for putative chemoeffectors in *P. aeruginosa*

To identify potential chemoeffectors for *P. aeruginosa*, we first screened chemical compounds from a large library of metabolites. Since several studies have shown correlation between a metabolic value of a compound and its potency as a chemoeffector (8, 37), we first used a growth assay to test effects of chemical compounds from three plates of the commercial Biolog compound arrays (PM1, PM2A and PM3B). This growth assay indeed showed that 202 compounds could be utilized as either carbon or nitrogen sources to support *P. aeruginosa* growth (Table S1). Out of those, we selected 30 compounds from Biolog compound arrays and additional 9 compounds that have been characterized as the specific ligands in other strains of *Pseudomonas* spp. These 39 compounds have not yet been characterized as chemoattractants for *P. aeruginosa*, indicating that at least some of them are likely to be novel ligands for *P. aeruginosa* chemoreceptors.

We next investigated the chemotactic responses of *P. aeruginosa* to these potential ligands by performing quantitative capillary chemotaxis assays (Fig. 1). Five compounds were able to highly

158 efficiently attract bacteria, with the strongest response being observed for methyl 4-
159 aminobutyrate, followed by 5-aminovalerate, ethanolamine (EA), L-ornithine, and 2-
160 phenylethylamine (PEA). Other seven compounds, guanine, glutarate, tricarballylate, niacinate,
161 succinate, fumarate and formate, acted as chemoattractants of intermediate strength. Of note, low
162 concentration of guanine (10 μM instead of 1 mM) was used in this assay due to its poor
163 solubility. The remaining compounds mediated only weak or no chemotaxis, despite being
164 nutrients.
165
166 **Construction of chimeras for 18 transmembrane chemoreceptors in *P. aeruginosa***
167 To investigate the specificities of these unassigned chemoeffectors, we focused on the 18
168 transmembrane chemoreceptors that belong to the F6 chemotaxis pathway of *P. aeruginosa*
169 (Table 1). To increase the probability of obtaining functional hybrid chemoreceptor for each
170 candidate, we applied three previously described construction strategies with different fusion
171 sites: within the transmembrane (TM) helix 2, after the HAMP domain, and within the TM2 helix
172 with a 5 amino acids random linker (17, 35). The resulting hybrids of type 1 and type 3 connect
173 the extracellular sensory domain, the TM1 helix, and part of the TM2 helix from *P. aeruginosa*
174 chemoreceptor to the rest of the TM2 helix, the HAMP domain and the cytoplasmic signaling
175 domain of *E. coli* chemoreceptor Tar (Fig. 2A). The fusion site of type 2 chimera is located in the
176 junction between the HAMP domain and cytoplasmic signaling domain, thus connecting the
177 extracellular sensory domain, the two TM helices and the whole HAMP domain from *P.*
178 *aeruginosa* chemoreceptor to the cytoplasmic signaling domain of Tar.
179

We subsequently tested the functionality of these chimeras expressed in a receptorless *E. coli* strain. We first used soft-agar gradient plates, where chemotactic cells exhibit biased spreading in gradients of compounds that are established by diffusion (Fig. 2B). Subsequently, we performed Förster resonance energy transfer FRET measurements (Fig. 2C) that are based on the phosphorylation-dependent interaction between CheY fused to yellow fluorescent protein (CheY-YFP) and CheZ fused to cyan fluorescent protein (CheZ-CFP). This assay enables to monitor activity of the chemotaxis pathway by following changes in the ratio YFP/CFP fluorescence, which is proportional to CheA activity (38). Because ligand specificity for many tested LBDs is not known, D-glucose was routinely used as a non-specific chemoattractant to assess the activity of hybrids. Differently from conventional chemoattractants, D-glucose is sensed via the phosphotransferase system (PTS) which signals to the cytoplasmic part of the chemoreceptor (39–41). A response to D-glucose thus demonstrates that the receptor hybrid activates the pathway and is responsive to stimulation, but the functionality of extracellular sensory domain and signal transduction toward the cytoplasmic part of the receptor remains to be confirmed by a specific ligand. From the constructed hybrids, only PA2561-Tar and PA4520-Tar showed no response to D-glucose. The functionality of several hybrids with already characterized LBDs was further verified by measuring FRET responses to their specific ligands (Table 1). Collectively, 16 active hybrid chemoreceptors were constructed successfully, and 7 of them were confirmed to be functional.

Screening of specific ligands for chemoreceptor chimeras using FRET

For these 16 functional hybrids, we conducted the one-by-one screening with potential ligands at a fixed concentration of 100 μM, using FRET measurements in *E. coli* strains expressing the indicated hybrid chemoreceptor as a sole chemoreceptor along with the CheZ-CFP/CheY-YFP FRET pair. A number of tested ligands elicited similar responses for all (or most) receptor hybrids, as well as for the full-length Tar (Table S2), indicating that these stimuli might be sensed by the cytoplasmic portion of Tar (2). Responses to other potential ligands were hybrid-specific, suggesting that their selectivity for a particular LBD (Table 1 and Table S2).

As an example, a hybrid that contains a 4HB-type LBD of PA1608 with unknown function showed not only responses to D-glucose but also similarly strong responses to inosine and guanine (Fig. 3A). These compounds did not stimulate Tar (Fig. S1A-C), suggesting that the extracellular sensor domain of PA1608 might be specific for inosine and guanine (see below). Another example is the hybrid with the LBD of PctB, a well-known amino acid chemoreceptor, where the response to L-glutamine was used to confirm its functionality. Different from Tar (Fig. S1B), PctB-Tar was also able to produce strong FRET response upon exposure to L-ornithine (Fig. 3B). Other identified ligands are summarized in Table 1 and Table S2. Besides purines and L-ornithine, these included methyl 4-aminobutyrate and 5-aminovalerate (specific to PctC) and salicylate (specific to PA2867).

In addition to molecular compounds, we tested the response to external pH that is also an important stimulus for bacterial chemotaxis receptors. Furthermore, several pH-active compounds present in the Biolog compound arrays used in our initial screening altered the pH of

the analysis buffer. We observed that several hybrids including PctA-Tar, PctB-Tar, PA1608-Tar and TlpQ-Tar mediated a repellent response to acidic pH 6.0 (Fig. 3), whereas PctC-Tar and PA1646-Tar showed an attractant response to acidic pH (Table S2). This indicates that, similar to that of *E. coli* (20), *P. aeruginosa* might exhibit bidirectional navigation in pH gradients in order to accumulate toward optimal pH.

Characterization of novel chemoeffectors for amino acid chemoreceptors PctA, PctB and PctC

In general, whenever clear responses to a particular ligand were observed in the micromolar concentration range in the *E. coli* FRET strain expressing chimera as a sole receptor, whereas the strain expressing wildtype Tar showed no response, it was seen as evidence that ligand is recognized by the respective sensory domain. The FRET results showed that, besides their known amino acid ligands, PctA-Tar and PctB-Tar were responsive to L-ornithine (Fig. 4A-C), whereas no response could be observed for Tar (Fig. S2A). This observation is consistent with a recent report, although direct binding of L-ornithine to these receptors was not demonstrated (42). We therefore performed ITC experiments using purified the LBDs of PctA and PctB, which confirmed binding of L-ornithine to both LBDs, with higher affinity (K_D = 7.1 μM) for PctA than for PctB (K_D = 559 μM) (Fig. 4D and E). This difference in affinity was consistent with the relative potency of these ligands as chemoeffectors for hybrids in *E. coli* (Fig. 4C), when taking into account the *in vivo* signal amplification by the *E. coli* chemotaxis system.

Similarly, the specificity of PctC-Tar response to methyl 4-aminobutyrate and 5-aminovalerate was confirmed by the dose-response FRET measurements (Fig. 5A-C and Fig. S2B-C). We further demonstrated direct binding of methyl 4-aminobutyrate (Fig. 5D) and 5-aminovalerate (Fig. 5E) to PctC-LBD by ITC, with dissociation constants of 129 and 28 μM, respectively. Again, these values were consistent with the higher sensitivity of PctC-Tar (lower EC50) to 5-aminovalerate in FRET measurements (Fig. 5C), taking in consideration the higher sensitivity of the *in vivo* response as discussed above. Finally, the relevance of the PctC-mediated response for chemotaxis of *P. aeruginosa* towards methyl 4-aminobutyrate and 5-aminovalerate was confirmed by the capillary chemotaxis assays, where the *pctC* deletion strain showed strongly reduced chemotaxis compared to the wildtype strain (Fig. 5F).

Characterization of PctP (PA1608) as a purine-specific chemoreceptor

The initial FRET screening showed that PA1608-Tar hybrid responded to guanine and inosine which are purine derivatives, whereas no responses were observed to cytosine, thymidine or uridine that all have a pyrimidine ring (Fig. 3A). Based on these observations, we speculated that PA1608 may be a purine-specific chemoreceptor. This hypothesis was further supported by TSA measurements of the binding of purine derivatives to PA1608, which all caused significant increases in the midpoint temperature of the protein unfolding transition (Fig. S3). We therefore further investigated the chemotactic responses of the PA1608-Tar hybrid to these 6 purine derivatives. When the PA1608-Tar hybrid was expressed as a sole chemoreceptor in *E. coli* FRET strain, clear attractant responses were observed to guanine and hypoxanthine in the lower micromolar range and to adenine at higher micromolar concentrations (Fig. 6A). Consistently,

responses were seen for *E. coli* strain expressing PA1608-Tar in gradients of guanine and hypoxanthine, but not of adenine, using the microfluidic chemotaxis assay (Fig. 6B). FRET responses were also observed for PA1608-Tar expressing cells to all three corresponding purine nucleosides (Fig. 6C). No responses to these purine derivatives were observed for the *E. coli* FRET strain and microfluidic strain expressing only the wild type Tar receptor (Fig. S2D-I and Fig. S4). Overall, the extracellular domain of PA1608 is most sensitive to the two nucleobases guanine and hypoxanthine, followed by the purine nucleosides and finally by adenine (Fig. 6D).

Additional evidence for the specificity of PA1608 for purines was obtained by ITC, which showed that PA1608-LBD binds to hypoxanthine with high affinity in a process characterized by negative cooperativity (K_{D1} = 43 μM and K_{D2} = 286 μM) (Fig. 6E), while the binding of guanine and other purine derivatives was not detected due to the limited solubility or low binding affinity. Since hypoxanthine was not included in our initial screen to identify novel chemoeffectors, we have generated the PA1608 mutant and performed capillary assays of chemotaxis to hypoxanthine using the wild type and the mutant strains. Indeed, the wild type cells showed strong chemoattractant response to 1 mM hypoxanthine, whereas the inactivation of the PA1608 chemoreceptor nearly abolished this response (Fig. 6F). Taken together, PA1608 responded with different sensitivity to 6 purine derivatives and was thus renamed as PctP (*Pseudomonas* chemotaxis transducer for purines).

Characterization of chemoreceptors for ethanolamine, 2-phenylethylamine and other biogenic amines

Two remaining strong chemoattractants, ethanolamine (EA) and 2-phenylethylamine (PEA), did not elicit apparent responses in our initial FRET screening. In order to identify their specific chemoreceptor(s), we screened receptor mutant strains of *P. aeruginosa* in the presence of 20 mM EA and PEA using quantitative capillary assays. Although no conclusive results were obtained for EA, a significant decrease in the chemoattraction to PEA was observed for the *tlpQ* mutant strain, and intermediate reduction for PA4915, PA1646 and PA4520 mutant strains (Fig. 7A), indicating that these receptors might play a role in the chemotaxis to PEA. This was supported by the thermal shift assays, which suggested that TlpQ-LBD and PA4915-LBD might bind PEA, and PA4915-LBD might also bind EA (Fig. 7B). In these cases, we were unable to observe clear FRET responses of TlpQ-Tar and PA4915-Tar hybrids to PEA or EA, although these two hybrids showed good responses to D-glucose (Table S2) and TlpQ-Tar mediated (weak) attractant responses to its known ligands such as histamine, spermidine and spermine (Fig. S5A). This suggests that TlpQ-Tar and PA4915-Tar hybrids are not fully functional, explaining why responses to PEA and EA were not detected in our initial FRET screen. Nevertheless, our ITC measurements confirmed the direct binding of PEA to TlpQ-LBD and PA4915-LBD (Fig. 7C and D). Collectively, despite poor functionality of their hybrids, we conclude that TlpQ and PA4915 are the major chemoreceptors for PEA chemotaxis in *P. aeruginosa*.

In previous studies, TlpQ was demonstrated to bind several biogenic amines, such as histamine, spermine, agmatine, cadaverine and putrescine (9). Since some of these compounds, as well as the newly identified ligand PEA, are produced by the decarboxylation of amino acids, we speculated that TlpQ might also sense tyramine, the decarboxylation product of tyrosine. Indeed, *tlpQ* mutant strain showed much reduced chemotaxis toward tyramine in the capillary assay (Fig. S5B), and binding of tyramine to TlpQ-LBD was confirmed by ITC (Fig. S5C).

311 Finally, we used FRET to test responses of amino acid chemoreceptors PctA, PctB and PctC to
312 histamine, one of the most important biogenic amines (43, 44). A recent study (9) suggested that
313 next to TlpQ, PctA and PctC also participate in the histamine chemotaxis, but microcalorimetric
314 titrations of the corresponding LBDs revealed only binding to TlpQ. In contrast, FRET
315 measurements confirmed that PctB and PctC can sense histamine in medium to high micromolar
316 range (Fig. S6), highlighting the advantage of using receptor hybrids for characterization of low-
317 affinity ligands.
318

319 **Discussion**

320 Bacteria contain an extensive array of different sensory receptors that respond to a variety of
321 stimuli, regulating multiple physiological functions including gene expression, chemotaxis or
322 second messenger signaling. Major receptor families include sensory histidine kinases,
323 chemoreceptors, adenylate, diadenylate and diguanylate cyclases and phosphodiesterases, as well
324 as Ser/Thr/Tyr protein kinases and phosphoprotein phosphatases (45). Typically, these receptors
325 are stimulated by the binding of signal molecules to their sensory domains that contain all the
326 requisites for ligand binding. However, the lack of established signals that are recognized by
327 receptors is currently a major bottleneck in our understanding of signal transduction processes in
328 bacteria (46).

329 The fact that the same type of sensor domain is frequently found in different signal transduction
330 systems suggests their modular nature and indicates that these domains have been exchanged
331 among different receptor families during evolution. This notion is exemplified by the dCache
332 domain that is the predominant type of the bacterial extracellular sensory domain, present in all

major bacterial receptor families (47). Previous success with construction of hybrid receptors (35, 36, 48, 49) confirmed this modularity and indicated that the exchange of sensory domains between different receptors can also be reproduced in the laboratory, and it is likely that such hybrid construction could be extended beyond chemoreceptor-chemoreceptor and chemoreceptor-sensor kinase hybrids to sensor domains from other types of receptors. Ligand screening for hybrid receptors, as done in this work, has thus the promise to become a universal approach to identify receptor ligands and thus to tackle a major bottleneck in microbiology.

Here we combined the screening based on hybrid chemoreceptors with binding and capillary assays to systematically identify novel ligands of chemoreceptors in *P. aeruginosa*, an important pathogen with a complex lifestyle and the correspondingly broad chemosensory range. Since many known bacterial chemoattractants are metabolically valuable compounds (8, 37), we first performed high-throughput screenings for candidate chemoeffectors using the growth assay, followed by an evaluation of their potency as chemoattractants for *P. aeruginosa* in the capillary chemotaxis assays. The strongest chemoattractants were then prioritized for further investigation using a library of hybrid chemoreceptors, containing the sensor domains of *P. aeruginosa* chemoreceptors fused to the signaling domain of *E. coli* Tar, to identify the potential ligand-receptor pairs using FRET and microfluidic assays (35). This approach has several advantages, including highly sensitive and standardized chemotaxis assays already established in *E. coli*, which enable detection not only of high- but also of low-affinity ligands, and testing not only binding of ligands but also their signaling properties. It further avoids the complication of functional redundancy between *P. aeruginosa* chemoreceptors with overlapping ligand specificities. Nevertheless, this hybrid-based *in vivo* screening also has some limitations, primarily because most but not all of the constructed hybrids are functional, and in those cases it

was complemented by *in vitro* ligand screening using TSA. Direct binding between the high-affinity ligands and sensor domains of chemoreceptors could further be confirmed using ITC. Finally, capillary chemotaxis assays were used to demonstrate the physiological relevance of identified ligand-receptor interactions for chemotaxis of *P. aeruginosa*.

This combination of assays enabled us to identify new ligands for previously studied chemoreceptors and to characterize new chemoreceptors in this well-studied model organism (Table 1). One example of the former category is the observed response to L-ornithine mediated by two amino acid chemoreceptors PctA and PctB, which support a recent study that implicated these receptors in *P. aeruginosa* chemotaxis towards L-ornithine (42). L-ornithine is a biologically versatile non-proteinogenic derivative of L-arginine. Besides its effects on growth, L-ornithine is known to promote of *P. aeruginosa* biofilm formation (50). L-ornithine might also accumulate in human lung environment during conditions that are associated with *P. aeruginosa* infections due to the elevated production of arginase (51), indicating a possible role of L-ornithine chemotaxis in virulence, and making its receptors potentially attractive target for therapeutic interventions. Indeed, the mutation of *pctA*, *pctB* and *pctC* reduced the accumulation of *P. aeruginosa* towards wounded lung epithelial cells (52). We observed that PctA senses L-ornithine at much lower concentrations than PctB, which is consistent with the previously observed difference in the sensitivity of these two receptors to L-arginine and several other amino acids (53). Another example is the *P. aeruginosa* response to other amino acid derivatives, methyl 4-aminobutyrate and 5-aminovalerate. We could show that these compounds are sensed by PctC, the high-affinity receptor for gamma-aminobutyric acid (GABA). This is consistent with

the structural similarity of these compounds to GABA, although their affinities to PctC are 10 to 100-fold lower than that of GABA (54).

Besides assigning new ligands to known chemoreceptors, we identified a novel purine-specific chemoreceptor PctP (PA1608). FRET results show that this receptor has highest affinity for guanine and hypoxanthine, intermediate affinity for purine nucleosides and significantly lower affinity for adenine, and it exhibits no response to pyrimidine derivatives. A lacking availability of nucleotide bases might limit growth of bacterial pathogens in the human host (55), including growth of *P. aeruginosa* in the lungs of cystic fibrosis (CF) patients (56), and cross-feeding of purine derivatives might play a role in a polymicrobial community in CF lungs (57). Thus, purine derivatives are both important nutrients and might be available during *P. aeruginosa* infection. Despite their potential importance, there are only few existing reports of chemotaxis towards purine or pyrimidine derivatives (11, 12, 58, 59), and only a single bacterial chemoreceptor specific for metabolizable purines has been characterized so far, McpH from *Pseudomonas putida* KT2440 (59). Interestingly, despite the phylogenetic proximity of *P. aeruginosa* and *P. putida*, McpH possesses a dCache-type LBD, whereas PctP has a four-helix bundle type LBD, indicative of convergent evolution (60) and providing further support to the important role of purine chemotaxis.

Finally, *P. aeruginosa* response to ethanolamine, 2-phenylethylamine and tyramine expands the ligand range of characterized chemoreceptors. TlpQ was previously reported to bind several biogenic amines (BAs), including putrescine, histamine, agmatine and cadaverine (9), which are derived from the decarboxylation of L-amino acids. BAs have important physiological functions in eukaryotic and prokaryotic cells, and many bacteria are able to produce and/or degrade BAs

(44, 61). Here, with PEA and tyramine we identified two additional TlpQ ligands. Sequence comparison between the dCache domain of TlpQ and the amino acid-binding dCache domains of PctA, PctB and PctC (62) shows conservation of amino acids that bind the amine group, which may explain the capacity of these receptor to bind either amino acids or their decarboxylated derivatives. Furthermore, we identified a second, previously uncharacterized, receptor PA4915 as a sensor of PEA, and possibly also of EA. The binding affinity of PA4915-LBD for PEA is even higher than that of TlpQ LBD, suggesting that it might be particularly important to mediate response to low concentrations of PEA. Notably, PA4915 possesses the four-helix bundle type LBD, which provides an interesting example of receptors within one bacterium that harbor different types of LBD but respond to the same ligand.

In addition to characterizing novel receptor specificities for chemical ligands, we observed that multiple LBDs of *P. aeruginosa* chemoreceptors can mediate specific responses to pH. In two model neutrophilic bacteria where pH taxis has been studied, *E. coli* (20) and *Bacillus subtilis* (19), bacterial accumulation toward neutral pH is ensured by opposite pH responses mediated by different receptors. In *E. coli*, the acidophilic response is primarily mediated by the LBD of Tar and the alkaliphilic response by the LBD of Tsr (20). Our results for the hybrid receptors suggest the existence of similar, but possibly more complex, bidirectional pH taxis in *P. aeruginosa*, with the LBDs of PctC and PA1646 mediating acidophilic taxis and those of PctB and PctP mediating alkaliphilic taxis. Particularly interesting are pH responses of the hybrids containing LBDs of PctA and TlpQ, which show repellent responses to both high and low pH, indicating that these receptors might even be individually able to mediate bacterial accumulation toward neutral pH. Given this multitude of pH responses mediated by the LBDs of *P. aeruginosa* chemoreceptors,

along with recently described general effects of pH on chemoreceptor LBDs (18), it would be interesting to investigate behavior of *P. aeruginosa* and other bacteria with complex chemosensory systems in pH gradients in future studies.

Taken together, our systematic screening strategy enabled us to enlarge the spectrum of ligand specificities of sensor domains in *P. aeruginosa*, despite it being already well-studied model for bacterial chemotaxis. A similar strategy could be applied for the systematic characterization of unknown sensor domains from different types of receptors in other species, including those that are unculturable.

Materials and methods

***Bacterial strains, plasmids and culture conditions*:** Bacterial strains and plasmids are listed in Table S3. For chemotaxis and FRET experiments, *E. coli* was grown in TB medium (1% tryptone and 0.5% NaCl) at 34 °C. For molecular cloning and protein expression, *E. coli* was grown in LB medium at 37 °C. *P. aeruginosa* was grown overnight in M9 minimal medium containing 15 mM D-glucose at 37 °C. When necessary, antibiotics were used at the following final concentrations: kanamycin, 50 µg/ml (*E. coli* strains); ampicillin, 100 µg/ml (*E. coli* strains); chloramphenicol, 34 µg/ml (*E. coli* strains) and 100 µg/ml (*P. aeruginosa* strains); tetracycline, 50 µg/ml (*P. aeruginosa* strains).

PA1608 mutant generation: To generate the *pctP* mutant strain, a 1280-bp fragment of PA1608 was amplified by PCR using primers PA1608_MUT_F and PA1608_MUT_R (Table S3). The

447 PCR product was cloned into pGEM®-T vector and transformed into *E. coli* DH5α. The resulting
448 plasmid pGEMT®-PA1608 was digested with ApaI and SpeI and the insert cloned into
449 pKNG101 previously digested with the same enzyme. The resulting plasmid pKNG101-PA1608
450 was then transformed into *E. coli* CC118 λpir. pKNG101_PA1608 was then introduced into *P.*
451 *aeruginosa* PAO1 by electroporation according to (63). The mutant was verified by PCR and
452 sequencing.
453
454 ***Growth assays:*** The analysis of the nutritional profile was carried out using the "Phenotype
455 Microarrays™" plates PM1, PM2A and PM3B (for further information, refer to
456 https://www.biolog.com/wp-content/uploads/2020/04/00A-042-Rev-C-Phenotype-MicroArrays-
457 1-10-Plate-Maps.pdf). Each of these plates contains 95 chemical compounds and one control
458 (H_2O). To determine the growth of *P. aeruginosa* using these compounds as the sole carbon or
459 nitrogen source, the lyophilized compounds present on the Biolog plates were resuspended in 90
460 µL of either M9 medium (for Biolog PM1 and PM2A plates) or M8 medium (M9 minimal
461 medium without NH_4Cl) containing 15 mM glucose (for Biolog PM3B plate). Subsequently, a *P.*
462 *aeruginosa* overnight culture was washed twice with M8 salts medium, diluted to an OD_{600} of 0.2
463 in M9 or M8 salts medium and then the wells with each of the compounds were inoculated with
464 10 µL of these cultures. Finally, growth was monitored at 37 ºC with shaking, determining the
465 OD_{600} every hour for 48 h in a Bioscreen Microbiological Growth Analyser (Oy Growth Curves
466 Ab Ltd, Helsinki, Finland).
467
468 ***Chemotaxis capillary assays for P. aeruginosa strains:*** Overnight cultures in M9 minimal
469 medium supplemented with 6 mg/L Fe-citrate, trace elements (64), and 15 mM glucose were used

to inoculate fresh medium to an OD_{660} of 0.05. Cells were cultured at 37 °C to an OD_{660} of 0.4. Subsequently, cells were washed twice by centrifugation (1,667 × g for 5 min) and resuspended in chemotaxis buffer (50 mM KH_2PO_4/K_2HPO_4, 20 mM EDTA, 0.05% [vol/vol] glycerol, pH 7.0). Aliquots (230 µl) of the cell suspension at an OD_{660} of 0.1. were placed into the wells of 96-well microtiter plates. Then, 1-µl capillaries (Microcaps, Drummond Scientific) were heat-sealed at one end and filled with buffer (control) or chemoeffector solution prepared in chemotaxis buffer. The capillaries were rinsed with sterile water and immersed into the bacterial suspensions at their open ends. After 30 min, capillaries were removed from the wells, rinsed with sterile water, and emptied into 1 ml of chemotaxis buffer. Serial dilutions were plated onto M9 minimal medium plates supplemented with 20 mM glucose, incubated at 37 °C prior to colony counting. Data were corrected with the number of cells that swam into buffer containing capillaries.

Construction of hybrid chemoreceptors: To construct the hybrid type 1 in a high-efficient way, the drop-out plasmid pHC8 was generated by Golden Gate Assembly kit (New England BioLabs), and the basic genetic parts are from Marburg collection (65). Dropout part served as placeholder, which carried a full expression cassette for the fluorescent proteins sfGFP to enable visible distinction of correct colonies and outward facing BsaI recognition sites. The signaling domain of Tar [198–553] was connected after the dropout part. The extracellular sensory domains of *P. aeruginosa* chemoreceptors containing BsaI recognition sites at both ends were synthesized, which allowed for replacing the dropout part by Golden Gate reaction, then generating the hybrid chemoreceptor in one-step reaction. For the constructions of hybrid type 2 and type 3, the coding sequences of each hybrid were amplified using PCR reaction (oligonucleotide sequences are shown in Table S3). The amplified fragments containing overlapping sequences of vector

493 pKG116 were ligated into the digested vector pKG116 using Gibson assembly reaction in
494 NEBuilder® HiFi DNA Assembly Master Mix (New England BioLabs). After cloning, the active
495 or functional hybrid type 3 were selected from a library of chemoreceptor[1–X]-XXXXX-[203–
496 553] as described previously (35) .
497
498 ***FRET measurements:*** FRET measurements were performed as described previously (35, 38, 66).
499 Cultures of the receptorless *E. coli* strain VS181 expressing chimeras of interest and CheY-
500 YFP/CheZ-CFP FRET pair were prepared by inoculating 200 µl of the overnight culture into 10
501 ml TB medium supplemented with appropriate antibiotics and inducers (50 µM isopropyl-β-D-
502 thiogalactoside (IPTG) and 1-2 µM sodium salicylate), and grown in a rotary shaker at 34°C and
503 275 rpm. Cells were harvested at OD_{600} of 0.5 by centrifugation, and washed twice with tethering
504 buffer (10 mM KH_2PO_4/K_2HPO_4, 0.1 mM EDTA, 1 µM methionine, 10 mM sodium lactate, pH
505 7.0). For microscopy, the cells were attached to the poly-lysine-coated coverslips for 10 min and
506 mounted into a flow chamber that was maintained under constant flow of 0.3 ml/min of tethering
507 buffer using a syringe pump (Harvard Apparatus) that was also used to add or remove
508 compounds of interest. The pH value of all tested compounds was adjusted to 7, except for
509 compounds that are only soluble under acidic or basic conditions, where the background buffer at
510 corresponding pH was tested as a negative control. FRET measurements were performed on an
511 upright fluorescence microscope (Zeiss AxioImager.Z1) equipped with photon counters
512 (Hamamatsu). The fluorescence signals were recorded and analyzed as described previously (17).
513
514 ***Protein overexpression and purification:*** The LBDs of chemoreceptors PctA, PctB, PctC,
515 PA4915 and TlpQ were purified as described previously (9, 67). For the remaining proteins, the

LBDs were cloned into a pET28b(+) expression vector. *E. coli* BL21 (DE3) harboring the LBD expression plasmid was grown in 5 L Erlenmeyer flasks containing 1 L LB medium supplemented with kanamycin under continuous stirring (200 rpm) at 37 °C. When OD_{600} reached 0.6, 0.1 mM isopropyl-β-D-thiogalactoside (IPTG) was added to induce protein expression. Growth was continued at 16 ºC for 12 h and cells were harvested by centrifugation at 10 000 x *g* for 30 min at 4 ºC. Proteins were purified by metal affinity chromatography using modified procedures for His GraviTrap™ column (Cytiva lifesciences, Marlborough, Massachusetts, USA). Briefly, cell pellets were resuspended in binding buffer (20 mM sodium phosphate, 500 mM NaCl, and 20 mM imidazole, pH 7.4) supplemented with 0.2 µg/ml lysozyme, 1 mM $MgCl_2$, 1 mM PMSF, stirred for 30 min at 4 ºC and lysed by an ultrasonic homogenizer for 10 min at 80 % amplitude (SONOPULS HD 4000; BANDELIN electronic GmbH & Co. KG, Berlin, Germany). After centrifugation at 20 000 x *g* for 30 min, the supernatant was loaded into His GraviTrap™ column pre-equilibrated with binding buffer, and target proteins were eluted by elution buffer (20 mM sodium phosphate, 500 mM NaCl, and 500 mM imidazole, pH 7.4). The protein fractions were dialyzed with the dialysis buffer (10 mM sodium phosphate, pH 5.5) to remove imidazole and NaCl, and concentrated using Amicon Ultra-15 centrifugal filters (Merck Millipore Ltd, Burlington, Massachusetts, USA).

Soft agar plate gradient assay for E. coli strains: To establish gradients, 200 µl aliquots of 100 mM chemical solutions were applied to the center line of minimal A agar plates (0.25% (w/v) agar, 10 mM KH_2PO_4/K_2HPO_4, 8 mM $(NH4)_2SO_4$, 2 mM citrate, 1 mM $MgSO_4$, 0.1 mg/ml of thiamine-HCl, 1 mM glycerol, and 40 µg/ml of a mixture of threonine, methionine, leucine, and histidine) supplemented with antibiotics and inducers and incubated overnight at 4 °C for

gradient formation. The receptorless *E. coli* cells expressing the chimera of interest as a sole receptor were grown overnight in 5 ml TB medium, harvested by centrifugation, washed by tethering buffer, resuspended in 200 µl tethering buffer, and applied to the plate at a 2.5 cm distance from the line where the chemical was inoculated. Plates were incubated at 30 °C for 24−48 hours.

The screening of active or functional hybrid type 3 containing a random linker was performed as described previously (35). The library of hybrids mixture was applied to an agar plate with D-glucose gradients for the three rounds of selection. Cells that accumulated at the edge of the colony ring were selected and re-inoculated for the second round of selection. After three rounds of selection, the best chemotactic cells were streaked out on LB plates to obtain single colonies. The chemotaxis behavior of the selected colonies was further confirmed on soft agar plates. The sequence of random linker for the functional hybrid was identified by DNA sequencing.

Microfluidic assays: The microfluidic assay was performed as previously described, using a chip with 24 parallel microchannels (68). The receptorless *E. coli* strain UU1250 expressing GFP and chimera of interest were grown at 34 °C in TB supplemented with antibiotics and inducers until OD_{600} of 0.5. Cells were harvested by centrifugation and washed twice with tethering buffer. The compounds of interest were dissolved in tethering buffer at a concentration of 50 mM and the pH was adjusted to 7.0. The chemical source microchannels were filled with 4 % (w/v) low-gelling temperature agarose to create a semi-permeable barrier. *E. coli* cells were added in the reservoir well and allowed to spread for 30 min into the channels. Compounds were added to the source well and allowed to form a concentration gradient. Cell fluorescence was recorded with a Nikon Ti-E inverted microscope system (Nikon Instruments Europe BV, Amsterdam, Netherlands)

562 using a 20x objective. Data were analyzed using ImageJ (Wayne Rasband, National Institutes of
563 Health, USA).
564
565 ***Thermal shift assays:*** Thermal shift assays were performed in 384 microtiter plates using a Bio-
566 Rad CFX384 Touch™ Real-Time PCR instrument with the presence or absence of potential
567 chemoattractants. Each 25 µl assay mixture contained 20.5 µl purified protein (30-100 µM) in
568 phosphate buffer (10 mM sodium phosphate, pH 5.5), 2 µl SYPRO™ orange (Invitrogen by
569 Thermo Fisher Scientific, Waltham, Massachusetts, USA) at 5 × concentration, and 2.5 µl 20 mM
570 potential chemoattractant. Samples were heated from 23 °C to 95 °C at a scan rate of 1 °C/min.
571 The protein unfolding curves were monitored by detecting changes in SYPRO™ Orange
572 fluorescence. The resulting data permitted the calculation of the mid-point of the protein
573 unfolding transition, or melting temperatures (Tm) using the first derivative values from the raw
574 fluorescence data, which was analyzed by the Bio-Rad CFX manager 3.1 software.
575
576 ***Isothermal titration calorimetry****:* Experiments were conducted on a VP-microcalorimeter
577 (Microcal, Amherst, MA, USA) at the temperatures indicated in Table S4. Proteins were dialyzed
578 into the buffer specified in Table S4 and placed into the sample cell. Ligand solutions were made
579 up in dialysis buffer at the concentrations indicated in Table S4 and titrated into the protein. The
580 mean enthalpies measured from the injection of ligands into buffer were subtracted from raw
581 titration data prior to data analysis with the MicroCal version of ORIGIN. Data were fitted with
582 the single-site binding model. In cases were data analysis with this model did not result in a
583 satisfactory fit, data were analyzed in SEDPHAT (69) using a model for the binding with
584 negative cooperativity to a macromolecule containing two symmetric sites.

Data availability:

All of the data are included in this article.

Acknowledgements:

This work was supported by the Max Planck Society and the Hessian Ministry of Higher Education, Research and the Arts (HMWK) – LOEWE research cluster "Diffusible Signals," subproject A1 (to VS), the Spanish Ministry for Science and Innovation/*Agencia Estatal de Investigación* 10.13039/501100011033 (grants PID2020-112612GB-I00 to TK and PID2019-103972GA-I00 to MAM) and the Junta de Andalucía (grant P18-FR-1621 to TK). JPCV was supported by the grant Unión Europea-NextGenerationEU RD 289/2021 UPM-Recualifica Margarita Salas. WX was supported by Peterson Group "Serving Hometown" Elites scholarship of Peterson Group Charity Foundation Limited and Chinese Scholarship Council (CSC) scholarship.

Abbreviations: FRET, Förster resonance energy transfer; ITC, isothermal titration calorimetry; LBD, ligand binding domain; TSA, thermal shift assays; PEA, 2-phenylethylamine; EA, ethanolamine; BAs, biogenic amines.

Conflict of interest: The authors do not declare any conflict of interest.

References

1. Sourjik V. and WNSV, Wingreen NS. 2012. Responding to chemical gradients: bacterial

chemotaxis. Curr Opin Cell Biol 24:194–225.

2. Bi S, Sourjik V. 2018. Stimulus sensing and signal processing in bacterial chemotaxis. Curr Opin Microbiol 45:22–29.

3. Keegstra JM, Carrara F, Stocker R. 2022. The ecological roles of bacterial chemotaxis. Nat Rev Microbiol 2022 208 20:491–504.

4. Colin R, Ni B, Laganenka L, Sourjik V. 2021. Multiple functions of flagellar motility and chemotaxis in bacterial physiology. FEMS Microbiol Rev 45:1–19.

5. Hazelbauer GL, Falke JJ, Parkinson JS. 2008. Bacterial chemoreceptors: high-performance signaling in networked arrays. Trends Biochem Sci.

6. Ortega Á, Zhulin IB, Krell T. 2017. Sensory Repertoire of Bacterial Chemoreceptors. Microbiol Mol Biol Rev 81.

7. Mesibov R, Adler J. 1972. Chemotaxis toward amino acids in *Escherichia coli*. J Bacteriol 112:315–326.

8. Yang Y, Pollard AM, Höfler C, Poschet G, Wirtz M, Hell R, Sourjik V. 2015. Relation between chemotaxis and consumption of amino acids in bacteria. Mol Microbiol 96:1272–1282.

9. Corral-Lugo A, Matilla MA, Martín-Mora D, Jiménez HS, Torres NM, Kato J, Hida A, Oku S, Conejero-Muriel M, Gavira JA, Krell T. 2018. High-Affinity Chemotaxis to Histamine Mediated by the TlpQ Chemoreceptor of the Human Pathogen Pseudomonas aeruginosa. MBio 9.

10. Matilla MA, Velando F, Tajuelo A, Martín-Mora D, Xu W, Sourjik V, Gavira JA, Krell T.

2022. Chemotaxis of the Human Pathogen *Pseudomonas aeruginosa* to the Neurotransmitter Acetylcholine. MBio 13.

11. Liu X, Parales RE. 2008. Chemotaxis of *Escherichia coli* to pyrimidines: a new role for the signal transducer tap. J Bacteriol 190:972–979.

12. Liu X, Wood PL, Parales J V., Parales RE. 2009. Chemotaxis to pyrimidines and identification of a cytosine chemoreceptor in *Pseudomonas putida*. J Bacteriol 191:2909–2916.

13. Martín-Mora D, Ortega A, Reyes-Darias JA, García V, López-Farfán D, Matilla MA, Krell T. 2016. Identification of a chemoreceptor in *Pseudomonas aeruginosa* that specifically mediates chemotaxis toward α-ketoglutarate. Front Microbiol 7.

14. Alvarez-Ortega C, Harwood CS. 2007. Identification of a malate chemoreceptor in *Pseudomonas aeruginosa* by screening for chemotaxis defects in an energy taxis-deficient mutant 73:7793–7795.

15. Adler J, Hazelbauer GL, Dahl MM. 1973. Chemotaxis toward sugars in *Escherichia coli*. J Bacteriol 115:824–847.

16. Matilla MA, Velando F, Martín-Mora D, Monteagudo-Cascales E, Krell T. 2022. A catalogue of signal molecules that interact with sensor kinases, chemoreceptors and transcriptional regulators. FEMS Microbiol Rev 46.

17. Bi S, Jin F, Sourjik V. 2018. Inverted signaling by bacterial chemotaxis receptors. Nat Commun 9.

18. Monteagudo-Cascales E, Martín-Mora D, Xu W, Sourjik V, Matilla MA, Ortega Á, Krell

T. 2022. The pH Robustness of Bacterial Sensing. MBio 13:e0165022.

19. Tohidifar P, Plutz MJ, Ordal GW, Rao C V. 2020. The mechanism of bidirectional pH taxis in *Bacillus subtilis*. J Bacteriol 202.

20. Yang Y, Sourjik V. 2012. Opposite responses by different chemoreceptors set a tunable preference point in *Escherichia coli* pH taxis. Mol Microbiol 86:1482–1489.

21. Yoney A, Salman H. 2015. Precision and variability in bacterial temperature sensing. Biophys J 108:2427–2436.

22. Paulick A, Jakovljevic V, Zhang S, Erickstad M, Groisman A, Meir Y, Ryu WS, Wingreen NS, Sourjik V. 2017. Mechanism of bidirectional thermotaxis in *Escherichia coli*. Elife 6.

23. Porter SL, Wadhams GH, Armitage JP. 2011. Signal processing in complex chemotaxis pathways. Nat Rev Microbiol 9:153–165.

24. Porter SL, Wadhams GH, Armitage JP. 2008. *Rhodobacter sphaeroides*: complexity in chemotactic signalling. Trends Microbiol 16:251–260.

25. Rao C V., Glekas GD, Ordal GW. 2008. The three adaptation systems of *Bacillus subtilis* chemotaxis. Trends Microbiol 16:480–487.

26. Ikuta KS, Swetschinski LR, Robles Aguilar G, Sharara F, Mestrovic T, Gray AP, Davis Weaver N, Wool EE, Han C, Gershberg Hayoon A, Aali A, Abate SM, Abbasi-Kangevari M, Abbasi-Kangevari Z, Abd-Elsalam S, Abebe G, Abedi A, Abhari AP, Abidi H, Aboagye RG, Absalan A, Abubaker Ali H, Acuna JM, Adane TD, Addo IY, Adegboye OA, Adnan M, Adnani QES, Afzal MS, Afzal S, Aghdam ZB, Ahinkorah BO, Ahmad A, Ahmad AR, Ahmad R, Ahmad S, Ahmad S, Ahmadi S, Ahmed A, Ahmed H, Ahmed JQ,

671 Ahmed Rashid T, Ajami M, Aji B, Akbarzadeh-Khiavi M, Akunna CJ, Al Hamad H,
672 Alahdab F, Al-Aly Z, Aldeyab MA, Aleman A V., Alhalaiqa FAN, Alhassan RK, Ali BA,
673 Ali L, Ali SS, Alimohamadi Y, Alipour V, Alizadeh A, Aljunid SM, Allel K, Almustanyir
674 S, Ameyaw EK, Amit AML, Anandavelane N, Ancuceanu R, Andrei CL, Andrei T,
675 Anggraini D, Ansar A, Anyasodor AE, Arabloo J, Aravkin AY, Areda D, Aripov T,
676 Artamonov AA, Arulappan J, Aruleba RT, Asaduzzaman M, Ashraf T, Athari SS, Atlaw D,
677 Attia S, Ausloos M, Awoke T, Ayala Quintanilla BP, Ayana TM, Azadnajafabad S, Azari
678 Jafari A, B DB, Badar M, Badiye AD, Baghcheghi N, Bagherieh S, Baig AA, Banerjee I,
679 Barac A, Bardhan M, Barone-Adesi F, Barqawi HJ, Barrow A, Baskaran P, Basu S, Batiha
680 AMM, Bedi N, Belete MA, Belgaumi UI, Bender RG, Bhandari B, Bhandari D, Bhardwaj
681 P, Bhaskar S, Bhattacharyya K, Bhattarai S, Bitaraf S, Buonsenso D, Butt ZA, Caetano dos
682 Santos FL, Cai J, Calina D, Camargos P, Cámera LA, Cárdenas R, Cevik M, Chadwick J,
683 Charan J, Chaurasia A, Ching PR, Choudhari SG, Chowdhury EK, Chowdhury FR, Chu
684 DT, Chukwu IS, Dadras O, Dagnaw FT, Dai X, Das S, Dastiridou A, Debela SA, Demisse
685 FW, Demissie S, Dereje D, Derese M, Desai HD, Dessalegn FN, Dessalegni SAA, Desye
686 B, Dhaduk K, Dhimal M, Dhingra S, Diao N, Diaz D, Djalalinia S, Dodangeh M,
687 Dongarwar D, Dora BT, Dorostkar F, Dsouza HL, Dubljanin E, Dunachie SJ, Durojaiye
688 OC, Edinur HA, Ejigu HB, Ekholuenetale M, Ekundayo TC, El-Abid H, Elhadi M,
689 Elmonem MA, Emami A, Engelbert Bain L, Enyew DB, Erkhembayar R, Eshrati B, Etaee
690 F, Fagbamigbe AF, Falahi S, Fallahzadeh A, Faraon EJA, Fatehizadeh A, Fekadu G,
691 Fernandes JC, Ferrari A, Fetensa G, Filip I, Fischer F, Foroutan M, Gaal PA, Gadanya MA,
692 Gaidhane AM, Ganesan B, Gebrehiwot M, Ghanbari R, Ghasemi Nour M, Ghashghaee A,
693 Gholamrezanezhad A, Gholizadeh A, Golechha M, Goleij P, Golinelli D, Goodridge A,

694 Gunawardane DA, Guo Y, Gupta R Das, Gupta S, Gupta VB, Gupta VK, Guta A,
695 Habibzadeh P, Haddadi Avval A, Halwani R, Hanif A, Hannan MA, Harapan H, Hassan S,
696 Hassankhani H, Hayat K, Heibati B, Heidari G, Heidari M, Heidari-Soureshjani R,
697 Herteliu C, Heyi DZ, Hezam K, Hoogar P, Horita N, Hossain MM, Hosseinzadeh M,
698 Hostiuc M, Hostiuc S, Hoveidamanesh S, Huang J, Hussain S, Hussein NR, Ibitoye SE,
699 Ilesanmi OS, Ilic IM, Ilic MD, Imam MT, Immurana M, Inbaraj LR, Iradukunda A, Ismail
700 NE, Iwu CCD, Iwu CJ, J LM, Jakovljevic M, Jamshidi E, Javaheri T, Javanmardi F,
701 Javidnia J, Jayapal SK, Jayarajah U, Jebai R, Jha RP, Joo T, Joseph N, Joukar F, Jozwiak
702 JJ, Kacimi SEO, Kadashetti V, Kalankesh LR, Kalhor R, Kamal VK, Kandel H, Kapoor N,
703 Karkhah S, Kassa BG, Kassebaum NJ, Katoto PD, Keykhaei M, Khajuria H, Khan A,
704 Khan IA, Khan M, Khan MN, Khan MA, Khatatbeh MM, Khater MM, Khayat Kashani
705 HR, Khubchandani J, Kim H, Kim MS, Kimokoti RW, Kissoon N, Kochhar S, Kompani F,
706 Kosen S, Koul PA, Koulmane Laxminarayana SL, Krapp Lopez F, Krishan K,
707 Krishnamoorthy V, Kulkarni V, Kumar N, Kurmi OP, Kuttikkattu A, Kyu HH, Lal DK,
708 Lám J, Landires I, Lasrado S, Lee S woong, Lenzi J, Lewycka S, Li S, Lim SS, Liu W,
709 Lodha R, Loftus MJ, Lohiya A, Lorenzovici L, Lotfi M, Mahmoodpoor A, Mahmoud MA,
710 Mahmoudi R, Majeed A, Majidpoor J, Makki A, Mamo GA, Manla Y, Martorell M, Matei
711 CN, McManigal B, Mehrabi Nasab E, Mehrotra R, Melese A, Mendoza-Cano O, Menezes
712 RG, Mentis AFA, Micha G, Michalek IM, Micheletti Gomide Nogueira de Sá AC,
713 Milevska Kostova N, Mir SA, Mirghafourvand M, Mirmoeeni S, Mirrakhimov EM,
714 Mirza-Aghazadeh-Attari M, Misganaw AS, Misganaw A, Misra S, Mohammadi E,
715 Mohammadi M, Mohammadian-Hafshejani A, Mohammed S, Mohan S, Mohseni M,
716 Mokdad AH, Momtazmanesh S, Monasta L, Moore CE, Moradi M, Moradi Sarabi M,

717 Morrison SD, Motaghinejad M, Mousavi Isfahani H, Mousavi Khaneghah A, Mousavi-
718 Aghdas SA, Mubarik S, Mulita F, Mulu GBB, Munro SB, Muthupandian S, Nair TS,
719 Naqvi AA, Narang H, Natto ZS, Naveed M, Nayak BP, Naz S, Negoi I, Nejadghaderi SA,
720 Neupane Kandel S, Ngwa CH, Niazi RK, Nogueira de Sá AT, Noroozi N, Nouraei H,
721 Nowroozi A, Nuñez-Samudio V, Nutor JJ, Nzoputam CI, Nzoputam OJ, Oancea B,
722 Obaidur RM, Ojha VA, Okekunle AP, Okonji OC, Olagunju AT, Olusanya BO, Omar Bali
723 A, Omer E, Otstavnov N, Oumer B, P A M, Padubidri JR, Pakshir K, Palicz T, Pana A,
724 Pardhan S, Paredes JL, Parekh U, Park EC, Park S, Pathak A, Paudel R, Paudel U, Pawar S,
725 Pazoki Toroudi H, Peng M, Pensato U, Pepito VCF, Pereira M, Peres MFP, Perico N,
726 Petcu IR, Piracha ZZ, Podder I, Pokhrel N, Poluru R, Postma MJ, Pourtaheri N, Prashant
727 A, Qattea I, Rabiee M, Rabiee N, Radfar A, Raeghi S, Rafiei S, Raghav PR, Rahbarnia L,
728 Rahimi-Movaghar V, Rahman M, Rahman MA, Rahmani AM, Rahmanian V, Ram P,
729 Ranjha MMAN, Rao SJ, Rashidi MM, Rasul A, Ratan ZA, Rawaf S, Rawassizadeh R,
730 Razeghinia MS, Redwan EMM, Regasa MT, Remuzzi G, Reta MA, Rezaei N, Rezapour A,
731 Riad A, Ripon RK, Rudd KE, Saddik B, Sadeghian S, Saeed U, Safaei M, Safary A, Safi
732 SZ, Sahebazzamani M, Sahebkar A, Sahoo H, Salahi S, Salahi S, Salari H, Salehi S,
733 Samadi Kafil H, Samy AM, Sanadgol N, Sankararaman S, Sanmarchi F, Sathian B,
734 Sawhney M, Saya GK, Senthilkumaran S, Seylani A, Shah PA, Shaikh MA, Shaker E,
735 Shakhmardanov MZ, Sharew MM, Sharifi-Razavi A, Sharma P, Sheikhi RA, Sheikhy A,
736 Shetty PH, Shigematsu M, Shin J Il, Shirzad-Aski H, Shivakumar KM, Shobeiri P, Shorofi
737 SA, Shrestha S, Sibhat MM, Sidemo NB, Sikder MK, Silva LMLR, Singh JA, Singh P,
738 Singh S, Siraj MS, Siwal SS, Skryabin VY, Skryabina AA, Socea B, Solomon DD, Song
739 Y, Sreeramareddy CT, Suleman M, Suliankatchi Abdulkader R, Sultana S, Szócska M,

740 Tabatabaeizadeh SA, Tabish M, Taheri M, Taki E, Tan KK, Tandukar S, Tat NY, Tat VY,
741 Tefera BN, Tefera YM, Temesgen G, Temsah MH, Tharwat S, Thiyagarajan A, Tleyjeh II,
742 Troeger CE, Umapathi KK, Upadhyay E, Valadan Tahbaz S, Valdez PR, Van den Eynde J,
743 van Doorn HR, Vaziri S, Verras GI, Viswanathan H, Vo B, Waris A, Wassie GT,
744 Wickramasinghe ND, Yaghoubi S, Yahya GATY, Yahyazadeh Jabbari SH, Yigit A, Yiğit
745 V, Yon DK, Yonemoto N, Zahir M, Zaman BA, Zaman S Bin, Zangiabadian M, Zare I,
746 Zastrozhin MS, Zhang ZJ, Zheng P, Zhong C, Zoladl M, Zumla A, Hay SI, Dolecek C,
747 Sartorius B, Murray CJL, Naghavi M. 2022. Global mortality associated with 33 bacterial
748 pathogens in 2019: a systematic analysis for the Global Burden of Disease Study 2019.
749 Lancet (London, England) 400:2221.

750 27. Ortega DR, Fleetwood AD, Krell T, Harwood CS, Jensen GJ, Zhulin IB. 2017. Assigning
751 chemoreceptors to chemosensory pathways in *Pseudomonas aeruginosa*. Proc Natl Acad
752 Sci U S A 114:12809–12814.

753 28. Matilla MA, Martín-Mora D, Gavira JA, Krell T. 2021. *Pseudomonas aeruginosa* as a
754 Model To Study Chemosensory Pathway Signaling. Microbiol Mol Biol Rev 85.

755 29. Kühn MJ, Talà L, Inclan YF, Patino R, Pierrat X, Vos I, Al-Mayyah Z, Macmillan H,
756 Negrete J, Engel JN, Persat A. 2021. Mechanotaxis directs *Pseudomonas aeruginosa*
757 twitching motility. Proc Natl Acad Sci U S A 118.

758 30. O'Neal L, Baraquet C, Suo Z, Dreifus JE, Peng Y, Raivio TL, Wozniak DJ, Harwood CS,
759 Parsek MR. 2022. The Wsp system of *Pseudomonas aeruginosa* links surface sensing and
760 cell envelope stress. Proc Natl Acad Sci U S A 119.

761 31. Kühn MJ, Macmillan H, Talà L, Inclan Y, Patino R, Pierrat X, Al-Mayyah Z, Engel JN,

762 Persat A. 2023. Two antagonistic response regulators control *Pseudomonas aeruginosa*
763 polarization during mechanotaxis. EMBO J https://doi.org/10.15252/EMBJ.2022112165.

764 32. Fernández M, Ortega Á, Rico-Jiménez M, Martín-Mora D, Daddaoua A, Matilla MA,
765 Krell T. 2018. High-throughput screening to identify chemoreceptor ligands. Methods Mol
766 Biol 1729:291–301.

767 33. Matilla MA, Martín-Mora D, Krell T. 2020. The use of isothermal titration calorimetry to
768 unravel chemotactic signalling mechanisms. Environ Microbiol 22:3005–3019.

769 34. Fernández M, Morel B, Corral-Lugo A, Rico-Jiménez M, Martín-Mora D, López-Farfán D,
770 Reyes-Darias JA, Matilla MA, Ortega Á, Krell T. 2016. Identification of ligands for
771 bacterial sensor proteins. Curr Genet 62:143–147.

772 35. Bi S, Pollard AM, Yang Y, Jin F, Sourjik V. 2016. Engineering Hybrid Chemotaxis
773 Receptors in Bacteria. ACS Synth Biol 5:989–1001.

774 36. Lehning CE, Heidelberger JB, Reinhard J, Nørholm MHH, Draheim RR. 2017. A Modular
775 High-Throughput in Vivo Screening Platform Based on Chimeric Bacterial Receptors.
776 ACS Synth Biol 6:1315–1326.

777 37. Fernández M, Matilla MA, Ortega Á, Krell T. 2017. Metabolic Value Chemoattractants
778 Are Preferentially Recognized at Broad Ligand Range Chemoreceptor of *Pseudomonas*
779 *putida* KT2440. Front Microbiol 8.

780 38. Sourjik V, Vaknin A, Shimizu TS, Berg HC. 2007. In vivo measurement by FRET of
781 pathway activity in bacterial chemotaxis. Methods Enzymol 423:365.

782 39. Somavanshi R, Ghosh B, Sourjik V. 2016. Sugar Influx Sensing by the Phosphotransferase

System of *Escherichia coli*. PLoS Biol 14.

40. Lux R, Jahreis K, Bettenbrock K, Parkinson JS, Lengeler JW. 1995. Coupling the phosphotransferase system and the methyl-accepting chemotaxis protein-dependent chemotaxis signaling pathways of *Escherichia coli*. Proc Natl Acad Sci U S A 92:11583–11587.

41. Neumann S, Grosse K, Sourjik V. 2012. Chemotactic signaling via carbohydrate phosphotransferase systems in *Escherichia coli*. Proc Natl Acad Sci U S A 109:12159–12164.

42. Dhodary B, Sampedro I, Behroozian S, Borza V, Her S, Hill JE. 2022. The Arginine Catabolism-Derived Amino Acid l-ornithine Is a Chemoattractant for P*seudomonas aeruginosa*. Microorganisms 10.

43. Doeun D, Davaatseren M, Chung MS. 2017. Biogenic amines in foods. Food Sci Biotechnol 26:1463.

44. Pugin B, Barcik W, Westermann P, Heider A, Wawrzyniak M, Hellings P, Akdis CA, O'Mahony L. 2017. A wide diversity of bacteria from the human gut produces and degrades biogenic amines. Microb Ecol Health Dis 28:1353881.

45. Galperin MY. 2018. What bacteria want. Environ Microbiol 20:4221.

46. Matilla MA, Monteagudo-Cascales E, Krell T. 2023. Advances in the identification of signals and novel sensing mechanisms for signal transduction systems. Environ Microbiol 25.

47. Upadhyay AA, Fleetwood AD, Adebali O, Finn RD, Zhulin IB. 2016. Cache Domains

That are Homologous to, but Different from PAS Domains Comprise the Largest Superfamily of Extracellular Sensors in Prokaryotes. PLoS Comput Biol 12.

48. Ravikumar S, David Y, Park SJ, Choi J il. 2018. A Chimeric Two-Component Regulatory System-Based *Escherichia coli* Biosensor Engineered to Detect Glutamate. Appl Biochem Biotechnol 186:335–349.

49. Kishii R, Falzon L, Yoshida T, Kobayashi H, Inouye M. 2007. Structural and functional studies of the HAMP domain of EnvZ, an osmosensing transmembrane histidine kinase in *Escherichia coli*. J Biol Chem 282:26401–26408.

50. Bernier SP, Ha DG, Khan W, Merritt JH, O'Toole GA. 2011. Modulation of *Pseudomonas aeruginosa* surface-associated group behaviors by individual amino acids through c-di-GMP signaling. Res Microbiol 162:680–688.

51. Maarsingh H, Pera T, Meurs H. 2008. Arginase and pulmonary diseases. Naunyn Schmiedebergs Arch Pharmacol 378:171–184.

52. Schwarzer C, Fischer H, Machen TE. 2016. Chemotaxis and Binding of *Pseudomonas aeruginosa* to Scratch-Wounded Human Cystic Fibrosis Airway Epithelial Cells. PLoS One 11.

53. Reyes-Darias JA, Yang Y, Sourjik V, Krell T. 2015. Correlation between signal input and output in PctA and PctB amino acid chemoreceptor of *Pseudomonas aeruginosa*. Mol Microbiol 96:513–525.

54. Reyes-Darias JA, García V, Rico-Jiménez M, Corral-Lugo A, Lesouhaitier O, Juárez-Hernández D, Yang Y, Bi S, Feuilloley M, Muñoz-Rojas J, Sourjik V, Krell T. 2015.

825 Specific gamma-aminobutyrate chemotaxis in pseudomonads with different lifestyle. Mol
826 Microbiol 97:488–501.

827 55. Samant S, Lee H, Ghassemi M, Chen J, Cook JL, Mankin AS, Neyfakh AA. 2008.
828 Nucleotide Biosynthesis Is Critical for Growth of Bacteria in Human Blood. PLoS Pathog
829 4.

830 56. Turner KH, Wessel AK, Palmer GC, Murray JL, Whiteley M. 2015. Essential genome of
831 *Pseudomonas aeruginosa* in cystic fibrosis sputum. Proc Natl Acad Sci U S A 112:4110–
832 4115.

833 57. Mahmud H Al, Baishya J, Wakeman CA. 2021. Interspecies Metabolic Complementation
834 in Cystic Fibrosis Pathogens via Purine Exchange. Pathogens 10:1–10.

835 58. Rahman H, King RM, Shewell LK, Semchenko EA, Hartley-Tassell LE, Wilson JC, Day
836 CJ, Korolik V. 2014. Characterisation of a Multi-ligand Binding Chemoreceptor CcmL
837 (Tlp3) of *Campylobacter jejuni*. PLoS Pathog 10:1003822.

838 59. Fernández M, Morel B, Corral-Lugo A, Krell T. 2016. Identification of a chemoreceptor
839 that specifically mediates chemotaxis toward metabolizable purine derivatives. Mol
840 Microbiol 99:34–42.

841 60. Gavira JA, Gumerov VM, Rico-Jiménez M, Petukh M, Upadhyay AA, Ortega A, Matilla
842 MA, Zhulin IB, Krell T. 2020. How Bacterial Chemoreceptors Evolve Novel Ligand
843 Specificities. MBio 11.

844 61. O'Donnell MP, Fox BW, Chao PH, Schroeder FC, Sengupta P. 2020. A neurotransmitter
845 produced by gut bacteria modulates host sensory behaviour. Nat 2020 5837816 583:415–

420.

62. Gumerov VM, Andrianova EP, Matilla MA, Page KM, Monteagudo-Cascales E, Dolphin AC, Krell T, Zhulin IB. 2022. Amino acid sensor conserved from bacteria to humans. Proc Natl Acad Sci U S A 119.

63. Choi KH, Kumar A, Schweizer HP. 2006. A 10-min method for preparation of highly electrocompetent Pseudomonas aeruginosa cells: Application for DNA fragment transfer between chromosomes and plasmid transformation. J Microbiol Methods 64:391–397.

64. Abril MA, Michan C, Timmis KN, Ramos JL. 1989. Regulator and enzyme specificities of the TOL plasmid-encoded upper pathway for degradation of aromatic hydrocarbons and expansion of the substrate range of the pathway. J Bacteriol 171:6782.

65. Stukenberg D, Hensel T, Hoff J, Daniel B, Inckemann R, Tedeschi JN, Nousch F, Fritz G. 2021. The Marburg Collection: A Golden Gate DNA Assembly Framework for Synthetic Biology Applications in Vibrio natriegens. ACS Synth Biol 10:1904–1919.

66. Sourjik V, Berg HC. 2002. Receptor sensitivity in bacterial chemotaxis. Proc Natl Acad Sci U S A 99:123–127.

67. Rico-Jiménez M, Muñoz-Martínez F, García-Fontana C, Fernandez M, Morel B, Ortega Á, Ramos JL, Krell T. 2013. Paralogous chemoreceptors mediate chemotaxis towards protein amino acids and the non-protein amino acid gamma-aminobutyrate (GABA). Mol Microbiol 88:1230–1243.

68. Si G, Yang W, Bi S, Luo C, Ouyang Q. 2012. A parallel diffusion-based microfluidic device for bacterial chemotaxis analysis. Lab Chip 12:1389–1394.

867 69. Zhao H, Piszczek G, Schuck P. 2015. SEDPHAT--a platform for global ITC analysis and
868 global multi-method analysis of molecular interactions. Methods 76:137–148.

869 70. Wu H, Kato J, Kuroda A, Ikeda T, Takiguchi N, Ohtake H. 2000. Identification and
870 characterization of two chemotactic transducers for inorganic phosphate in *Pseudomonas*
871 *aeruginosa*. J Bacteriol 182:3400–3404.

872 71. Rico-Jiménez M, Reyes-Darias JA, Ortega Á, Diez Pena AI, Morel B, Krell T. 2016. Two
873 different mechanisms mediate chemotaxis to inorganic phosphate in *Pseudomonas*
874 *aeruginosa*. Sci Rep 6.

875 72. Martín-Mora D, Ortega Á, Matilla MA, Martínez-Rodríguez S, Gavira JA, Krell T. 2019.
876 The molecular mechanism of nitrate chemotaxis via direct ligand binding to the PilJ
877 domain of MCPN. MBio 10:1–17.

878

879

880

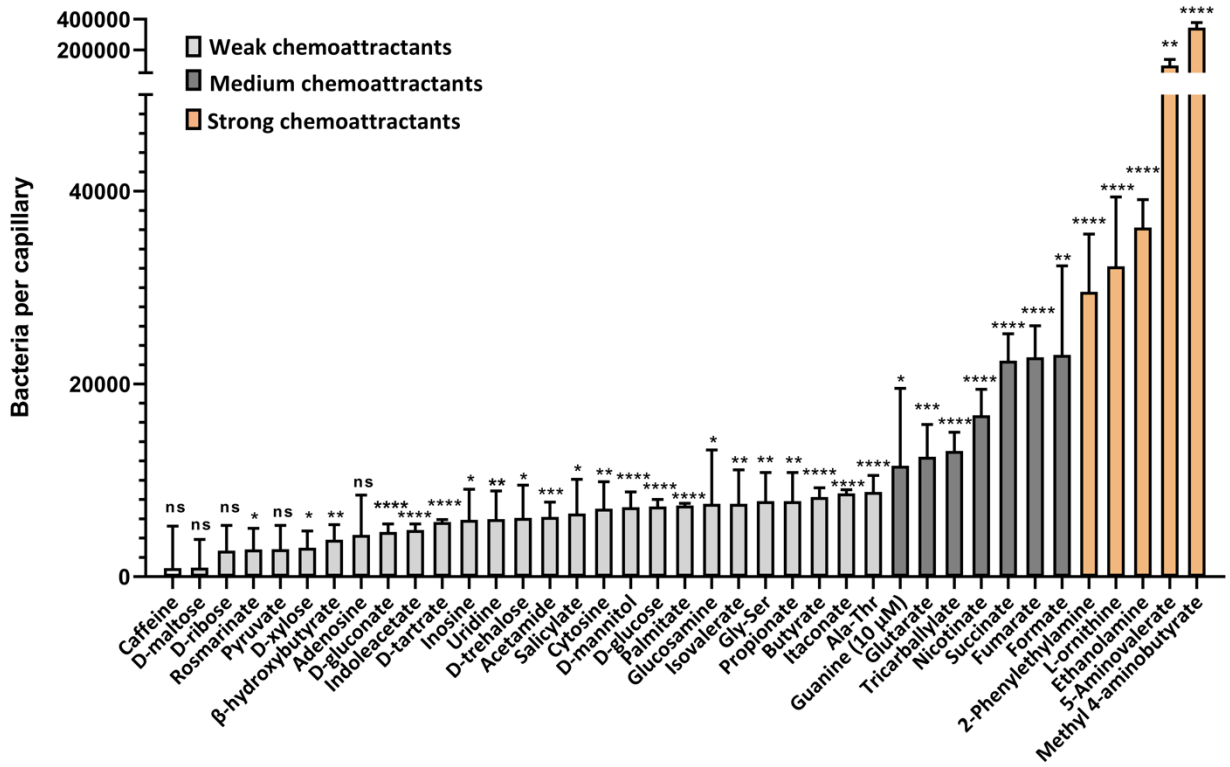

881

882 **Fig. 1 Chemotaxis of *P. aeruginosa* PAO1 toward potential chemoeffectors.** Accumulation of bacteria (WT-
883 Washington) in capillaries containing 1 mM of indicated chemical compound in the chemotaxis buffer, except
884 guanine that was used at 10 µM due to poor solubility. Strong chemoattractants with >30,000 cells per capillary are
885 shown in orange; medium chemoattractants with 10,000 - 30,000 cells per capillary are shown in dark grey and the
886 remaining chemical compounds are shown in light grey. All data have been corrected by the number (7,825 ± 623) of
887 bacteria in buffer-containing capillaries. The means and standard deviations of four biological replicates each
888 conducted in triplicate are shown. Error bars indicate the mean ± standard deviations. Significance of difference was
889 statistically significant differences from buffer-containing capillaries, assessed using an unpaired Student's t-test, are
890 indicated by asterisks (ns: non-significant, *$p \leq 0.05$, **$p \leq 0.01$, ***$p \leq 0.001$, and ****$p \leq 0.0001$).

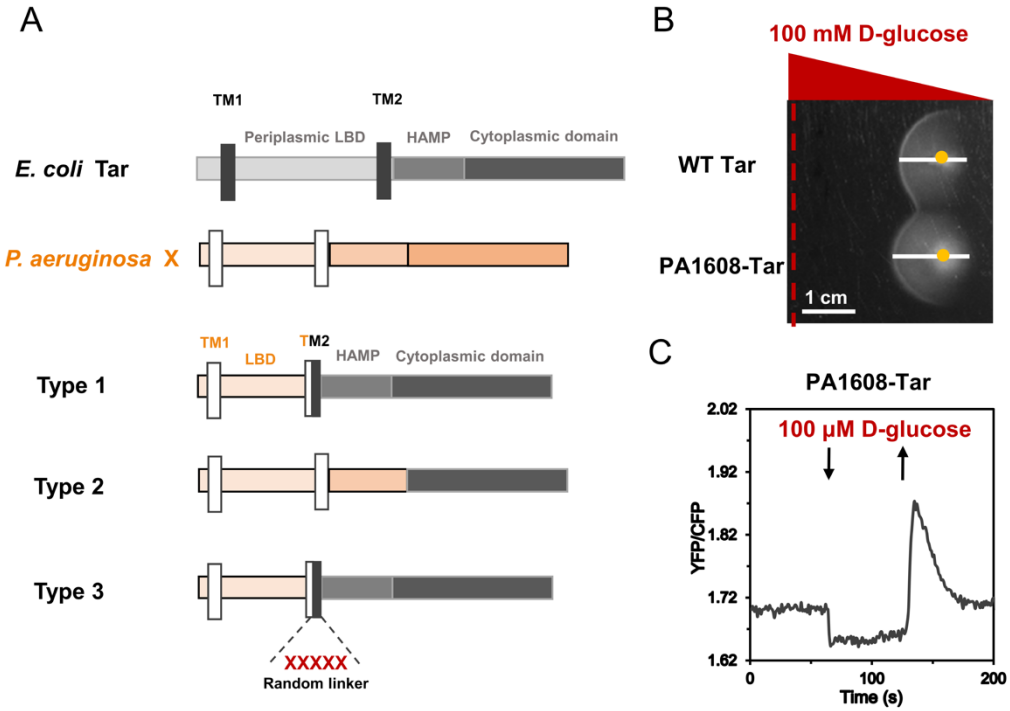

Fig. 2 Construction and evaluation of receptor hybrids for transmembrane chemoreceptors of *P. aeruginosa* PAO1. (A) Schematic drawing of three types of hybrid chemoreceptors constructed in this work. Tar chemoreceptor from *E. coli* and target chemoreceptor (X) from *P. aeruginosa* each consist of three parts, periplasmic ligand binding domain, HAMP domain and cytoplasmic domain, shown in different colors. The two TM helices are shown by black and white rectangles in the Tar receptor and the target chemoreceptor (X), respectively. (B) D-glucose gradient plate assay used for the assessment of receptor functionality. The control was the receptorless *E. coli* cells expressing wildtype Tar as the sole receptor. Positions of the ligand source and inoculated cells are shown by a red dotted line and by a yellow dot, respectively. Spreading of cells toward or away from the ligand source is indicated by the white line (scale bar, 1 cm). (C) FRET measurement of the hybrid chemoreceptor response to D-glucose. Receptorless *E. coli* cells expressing the CheZ-CFP/CheY-YFP FRET pair and PA1608-Tar as the sole receptor responded to stepwise addition (down arrow) and subsequent removal (up arrow) of the 100 μM D-glucose. Similar to canonical chemoattractants, addition of D-glucose inhibits pathway activity and thus lowers the YFP/CFP fluorescence ratio.

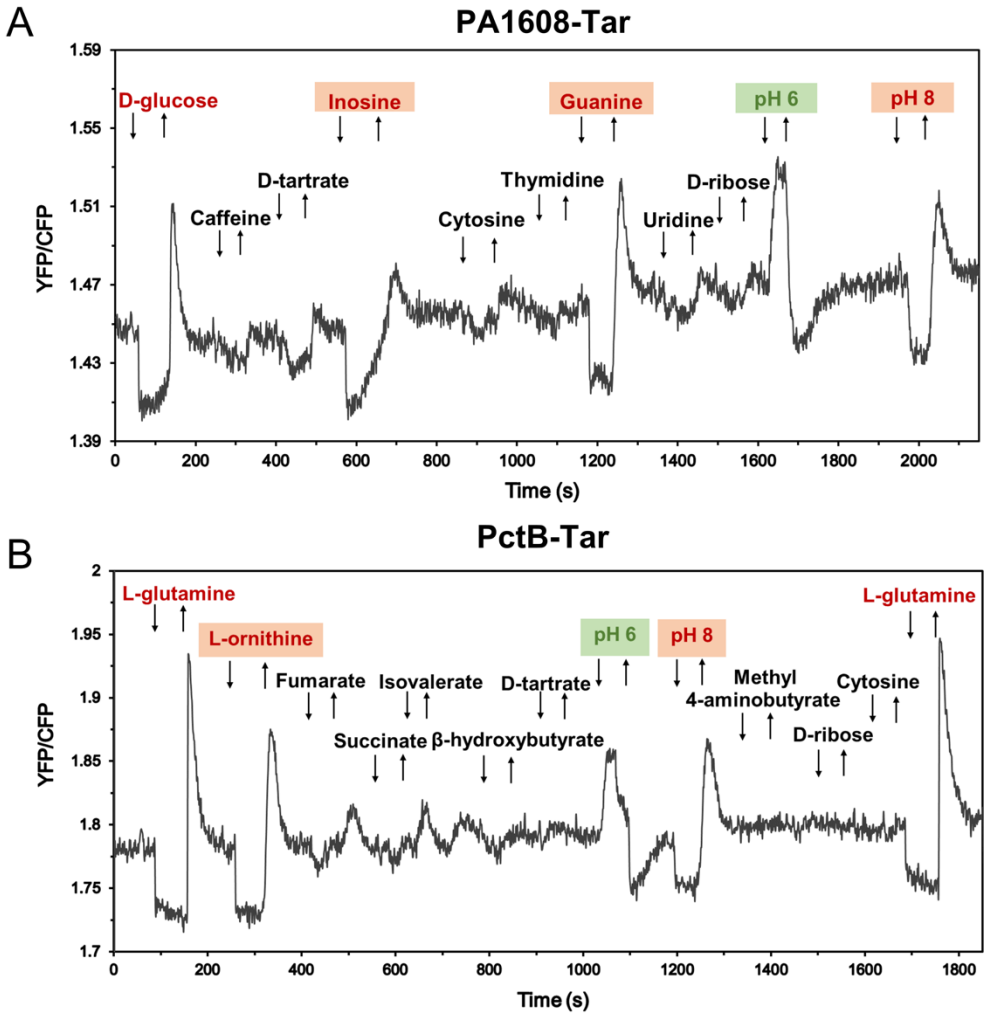

905

906 **Fig. 3 High-throughput screening of unassigned potential ligands for chemoreceptor chimeras with FRET.**
907 Examples of FRET measurements of receptorless *E. coli* FRET strain expressing PA1608-Tar (A) or PctB-Tar (B) as
908 the sole receptor, responding to the stepwise addition (down arrow) and subsequent removal (up arrow) of indicated
909 chemical compounds at concentration of 100 μM. Because of lack of previously characterized ligand for PA1608, D-
910 glucose was used as a positive control for PA1608-Tar hybrid during FRET measurements to confirm receptor
911 functionality. L-glutamine was used as a positive ligand for PctB-Tar hybrid. The chemoattractants are indicated in
912 red and the chemorepellents were shown in green; newly identified chemoeffectors are shaded.

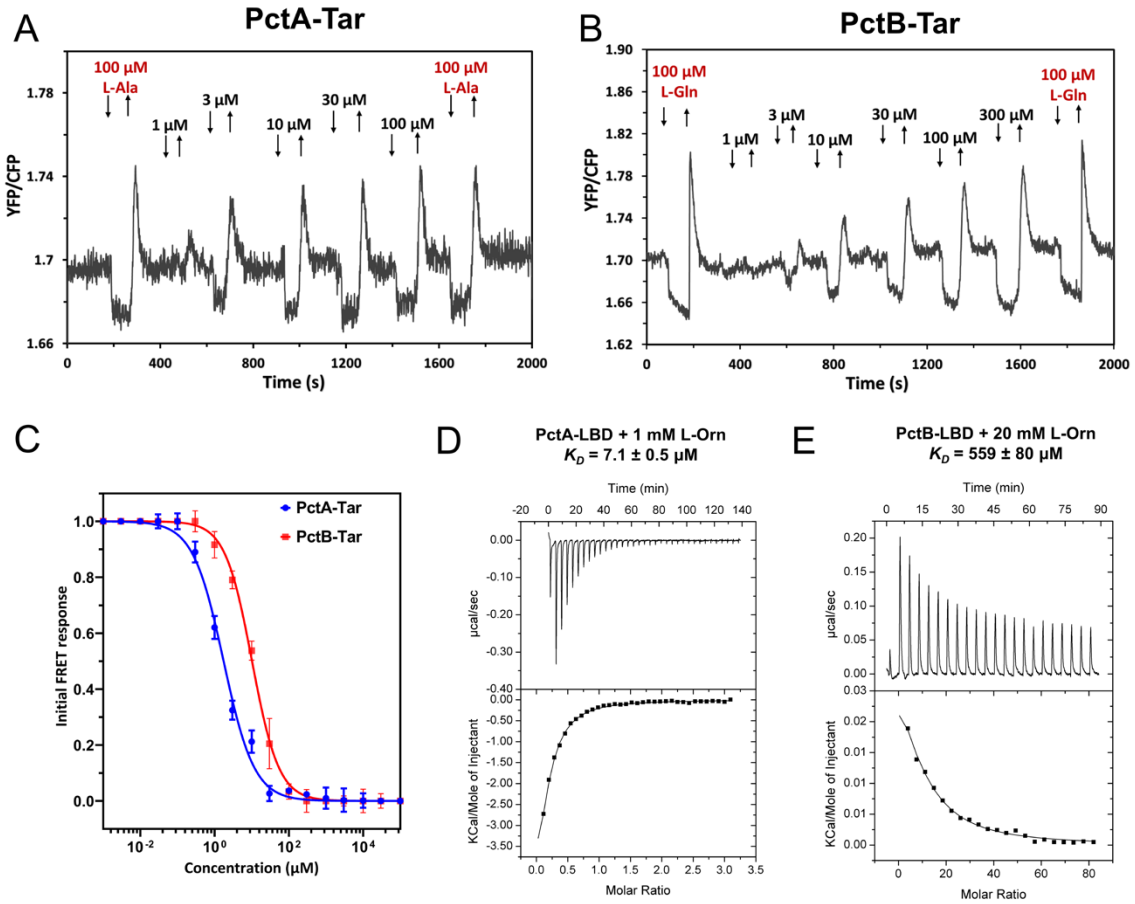

Fig. 4 Characterization of L-ornithine sensing by PctA and PctB *in vivo* and *in vitro*. (A-C) FRET measurements of response to the indicated concentrations of L-ornithine (L-Orn) in *E. coli* expressing PctA-Tar (A) or PctB-Tar (B) as a sole receptor. The known ligands L-Ala (L-alanine) and L-Gln (L-glutamine) were used as positive controls for PctA-Tar and PctB-Tar, respectively. For corresponding dose-response curves (C), the amplitudes of the initial FRET response were calculated from changes in the ratio of YFP/CFP fluorescence after stimulation with indicated ligand concentrations and normalized to the saturated response. Error bars indicate the standard errors of three independent experiments; wherever invisible, error bars are smaller than the symbol size. Data were fitted using Hill equation, with the EC50 fit values being 1.8 ± 0.2 μM for PctA-Tar and 10.2 ± 0.8 μM for PctB-Tar. (D, E) Microcalorimetric titrations of PctA-LBD (D) and PctB-LBD (E) with L-Orn. The upper panels show raw titration data, and lower panels show integrated corrected peak areas of the titration data fit using the single-site binding model. Further experimental detail is provided in Table S4.

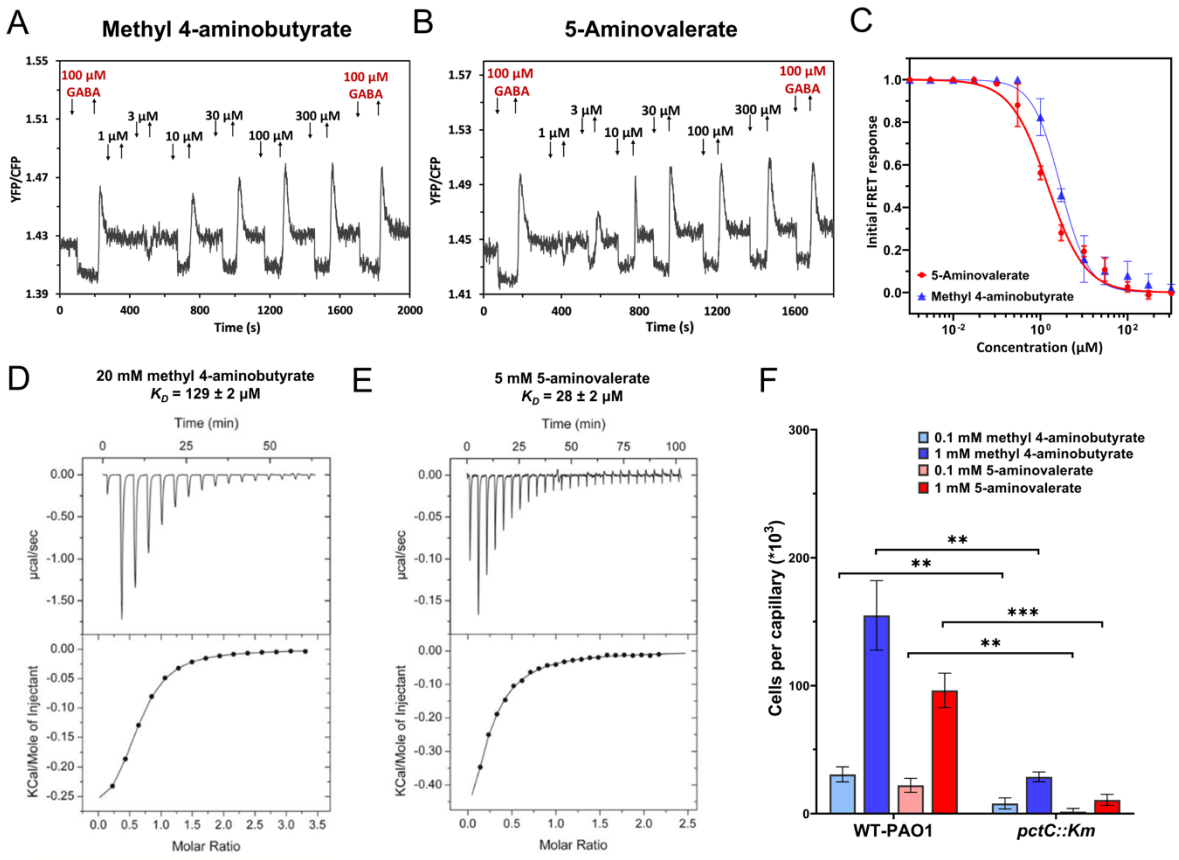

Fig. 5 Characterization of PctC as a specific chemoreceptor for methyl 4-aminobutyrate and 5-aminovalerate. FRET measurements for *E. coli* cells expressing PctC-Tar hybrid as a sole receptor to the indicated concentrations of methyl 4-aminobutyrate (A) and 5-aminovalerate (B). The known ligand GABA (γ-Aminobutyric acid) was used as a positive ligand. (C) Corresponding FRET dose-response curves of PctC-Tar hybrid to methyl 4-aminobutyrate and 5-aminovalerate. Data were fitted using Hill equation, with the EC50 fit values being 2.9 ± 0.4 µM for methyl 4-aminobutyrate, and 1.5 ± 0.2 µM for 5-aminovalerate. The measurement and data analysis were conducted as described in the Fig. 4C. Microcalorimetric titrations of PctC-LBD with methyl 4-aminobutyrate (D) and 5-aminovalerate (E). The upper panel upper shows raw titration data, and lower shows integrated corrected peak areas of the titration data fit using the single-site binding model. (F) Capillary chemotaxis assays of the wildtype *P. aeruginosa* (WT-Hiroshima) and a *pctC* mutant strain (WT-Hiroshima was used as the parental strain) response to methyl 4-aminobutyrate and 5-aminovalerate. Data are shown as the means and standard deviations of results from three biological replicates each conducted in triplicate. Asterisks denote statistically significant differences; ns: non-significant, * $p \leq 0.05$, ** $p \leq 0.01$, *** $p \leq 0.001$, **** $p \leq 0.0001$.

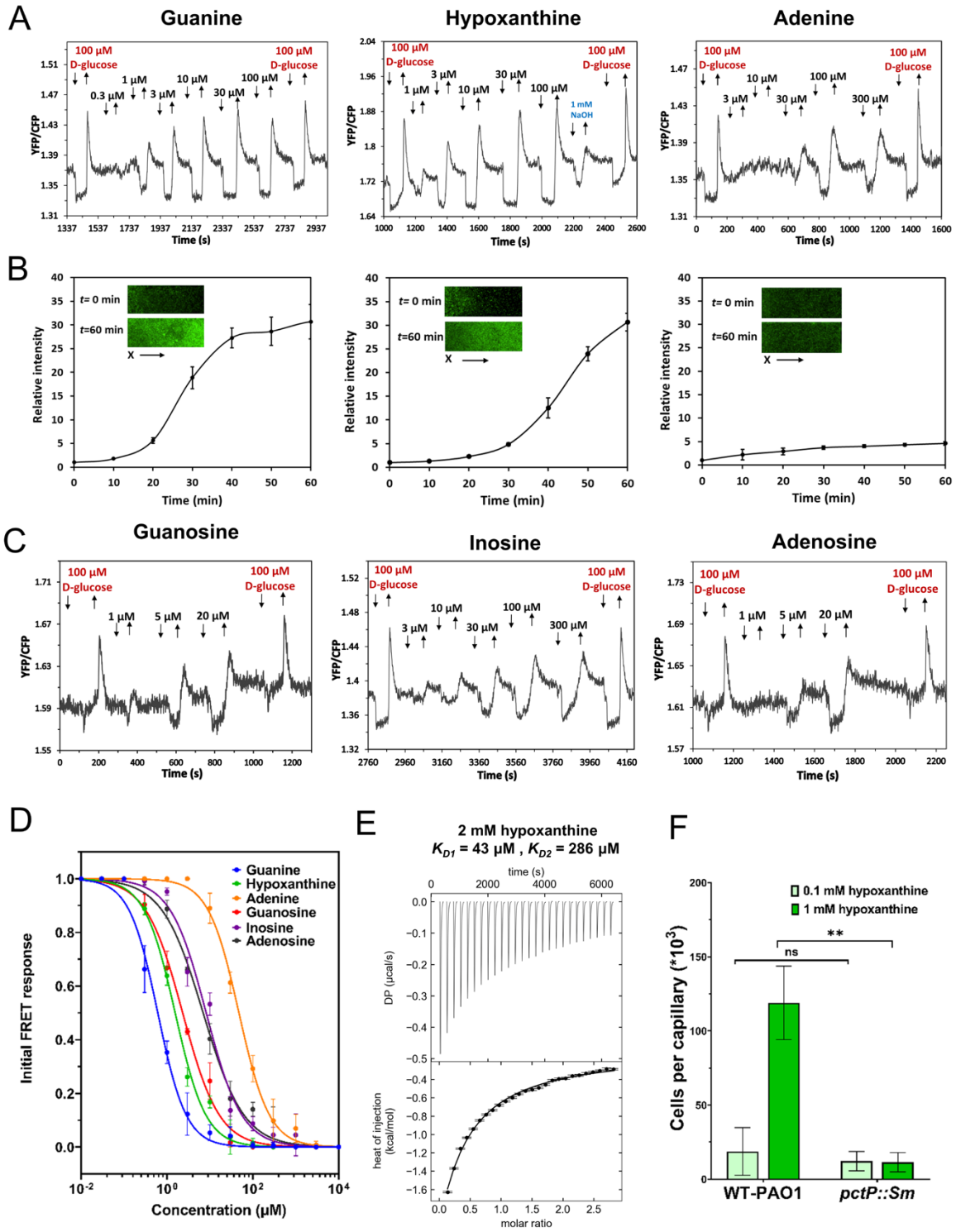

939

940 **Fig. 6 Characterization of PA1608 (PctP) as a purine-specific chemoreceptor.** (A) FRET measurements for *E.*

941 *coli* cells expressing PctP-Tar hybrid as a sole receptor to the indicated concentrations of guanine, hypoxanthine, and

942 adenine. Since there is no previously characterized ligand for PctP, D-glucose was used as a positive control. The

stock solutions of guanine and hypoxanthine were prepared with NaOH due to their poor solubility in neutral pH, and consequently 1 mM NaOH was used as control to exclude the influence of pH on the response of PctP-Tar hybrid. (B) Microfluidic assay of the chemotactic response of *E. coli* expressing PctP-Tar as the sole receptor and GFP as a label. Relative cell density (fluorescence intensity of GFP) in the observation channel over time in gradients of guanine, hypoxanthine, or adenine in the same order as in (A), with 50 mM in the source channel as indicated. Cell density in the observation channel before ligands stimulation (t=0) was used to normalize all data. Error bars indicate standard deviation from three independent biological replicates. Inserts show representative images of the observation channel at the beginning and the end of an experiment. The x-components (black arrow) indicate the direction up the concentration gradient. (C) FRET measurements as in (A) but for guanosine, inosine, and adenosine. (D) Dose-response curves for FRET measurements of responses mediated by PctP-Tar. Data were fitted using Hill equation, with the EC50 fit values being 0.6 ± 0.1 μM for guanine, 1.6 ± 0.2 μM for hypoxanthine, 47.6 ± 4.1 μM for adenine, 2.3 ± 0.3 μM for guanosine, 8.2 ± 1.9 μM for inosine, and 7.0 ± 1.3 μM for adenosine. The measurement and data analysis were conducted as described in Fig. 4C. (E) Microcalorimetric titrations of PctP-LBD with hypoxanthine. The upper panel shows the titration raw data, and the lower panel is the integrated dilution heat corrected and concentration normalized peak areas fitted with model for the binding with negative cooperativity to two symmetric sites. (F) Capillary chemotaxis assays of WT-PAO1 and a *pctP* mutant to 0.1 mM and 1 mM hypoxanthine. The *pctP* mutant was derived from the Washington parental strain that was used as a WT-PAO1 in this measurement. Data are shown as the means and standard deviations from three biological replicates each conducted in triplicate. Asterisks denote statistically significant differences; ns: non-significant, * $p \leq 0.05$, ** $p \leq 0.01$, *** $p \leq 0.001$, **** $p \leq 0.0001$.

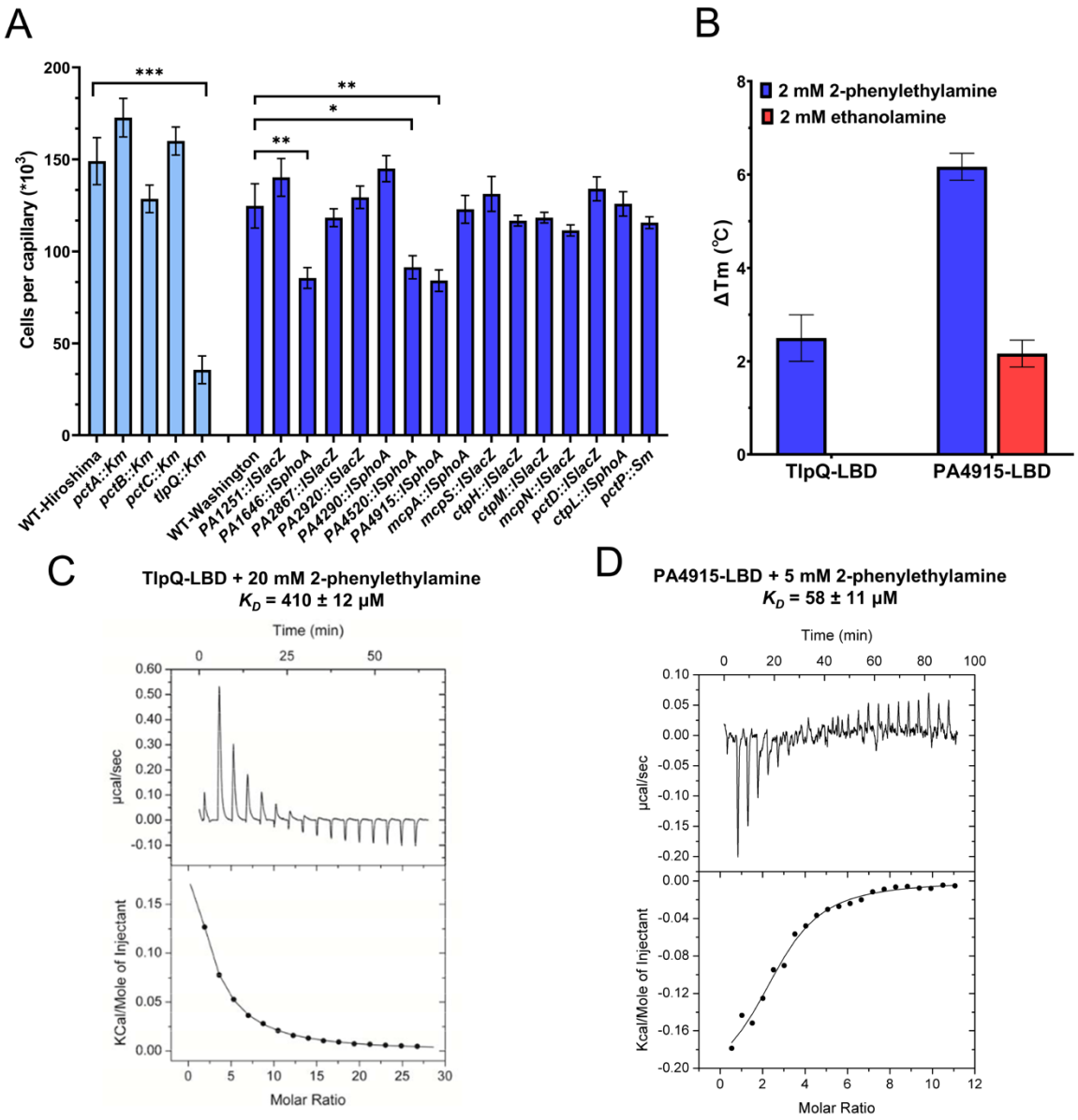

963

964 **Fig. 7 Identification of specific chemoreceptors for ethanolamine and 2-phenylethylamine.** (A) Capillary assay
965 for chemotaxis toward 20 mM 2-phenylethylamine (PEA) in different chemoreceptor mutants of PAO1. Mutant
966 strains deficient in PctA, PctB, PctC and TlpQ were derived from WT-Hiroshima parental strain (shown in light blue)
967 which was used as a reference. The remaining mutant strains were derived from WT-Washington parental strain
968 (shown in blue) which was used as a reference for these mutants. Data are shown as the means and standard
969 deviations of results from three biological replicates each conducted in triplicate. Asterisks denote statistically
970 significant differences; ns: non-significant, * $p \leq 0.05$, ** $p \leq 0.01$, *** $p \leq 0.001$, **** $p \leq 0.0001$. (B) Thermal

971 shift assay for TlpQ-LBD and PA4915-LBD in presence of 2 mM PEA or ethanolamine (EA). Data are shown as the
972 means and standard deviations of results from three biological replicates each conducted in triplicate. (C, D)
973 Microcalorimetric titrations of TlpQ-LBD (C) and PA4915-LBD (D) with PEA. Upper panels show raw titration
974 data, whereas lower panels show the best fit of the integrated, concentration-normalized and dilution heat corrected
975 raw data using the single-site binding model.

976

977

978 **Table 1.** Summary of all the chimeras constructed and new chemoeffectors identified in this work

Locus tag	Name[a]	LBD type	Hybrid type[b]	Known chemoeffectors[c]	New chemoeffectors
PA2654	TlpQ[9]	dCache	T1	Histamine, +	2-Phenylethylamine, tyramine
PA4915		4HB	T1		2-Phenylethylamine
PA4844	CtpL[70, 71]	HBM	T1	Inorganic phosphate	
PA2573		4HB	T1		
PA2788	McpN[72]	PilJ	T1	Nitrate	
PA1608		4HB	T1, T2		Guanine, inosine, adenosine, hypoxanthine, adenine, guanosine
PA4310	PctB[53, 67]	dCache	T1, T2[53]	L-glutamine (L-Gln), +	L-ornithine (L-Orn)
PA4309	PctA[53, 67]	dCache	T1, T2[53]	L-alanine (L-Ala), +	L-ornithine (L-Orn)
PA4307	PctC[54, 67]	dCache	T1, T2[54]	γ-Aminobutyric acid (GABA), +	5-Aminovalerate, methyl 4-aminobutyrate
PA4633	PctD[10]	dCache	T1, T2[10]	Acetylcholine, +	
PA2652	CtpM[14]	sCache	T1, T2	Malate, +	
PA5072	McpK[13]	HBM	T1, T3	α-Ketoglutarate, +	
PA2867		Unknown	T1, T3		Salicylate
PA2920		4HB	T1, T3		
PA1251		4HB	T1, T3		
PA1646		HBM	T1, T3		
PA2561	CtpH[70, 71]	4HB	T1, T3	Inorganic phosphate	
PA4520		NIT	T1, T3		

979 [a]Specificities of several chemoreceptors have been identified in the indicated references.

980 [b]T1: Type 1 is a hybrid chemoreceptor with fusion site within TM2; T2: Type 2 has fusion site at the end of HAMP domain; T3:
981 Type 3 has the same fusion site as type 1, but contains in addition a random linker of 5 amino acids. The hybrid type of chimera
982 that respond to D-glucose is highlighted in black, with grey marking hybrids that did not show a response. Functional hybrid
983 chemoreceptors that have been described previously, with the references provided in brackets.

984 [c]Previously identified specific ligands, with "+" indicating that the hybrid chemoreceptor was able to mediate FRET response to
985 this ligand.

986

Supplementary Data

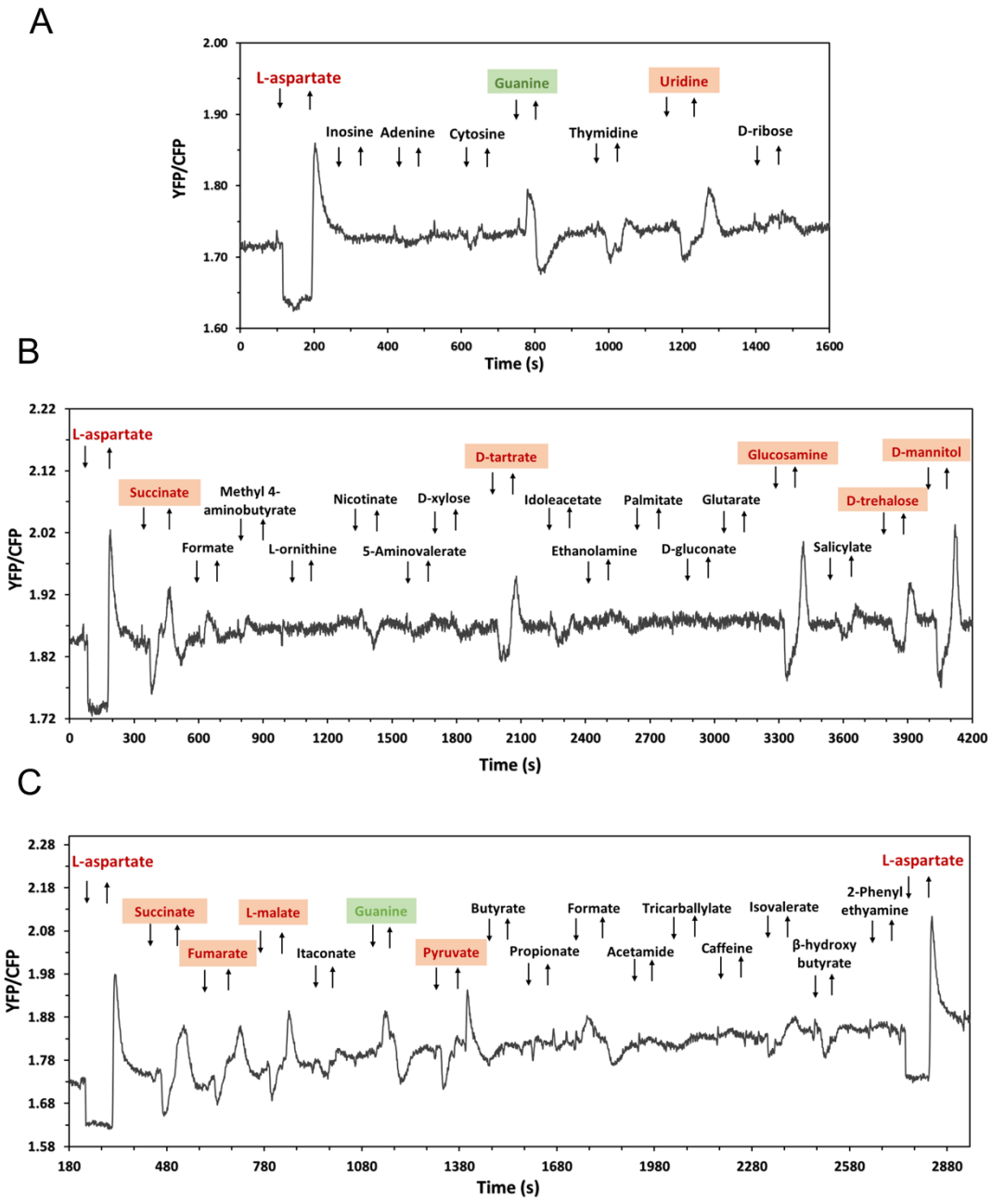

Fig. S1 Responses of Tar control to unassigned potential ligands. FRET measurements of responses in receptorless *E. coli* cells expressing wildtype Tar as the sole receptor, stimulated by the stepwise addition (down arrow) and subsequent removal (up arrow) of 100 μM L-aspartate (L-Asp, positive ligand for Tar) or other tested compounds, as indicated. The chemoattractants are shown in red and the chemorepellents are shown in green.

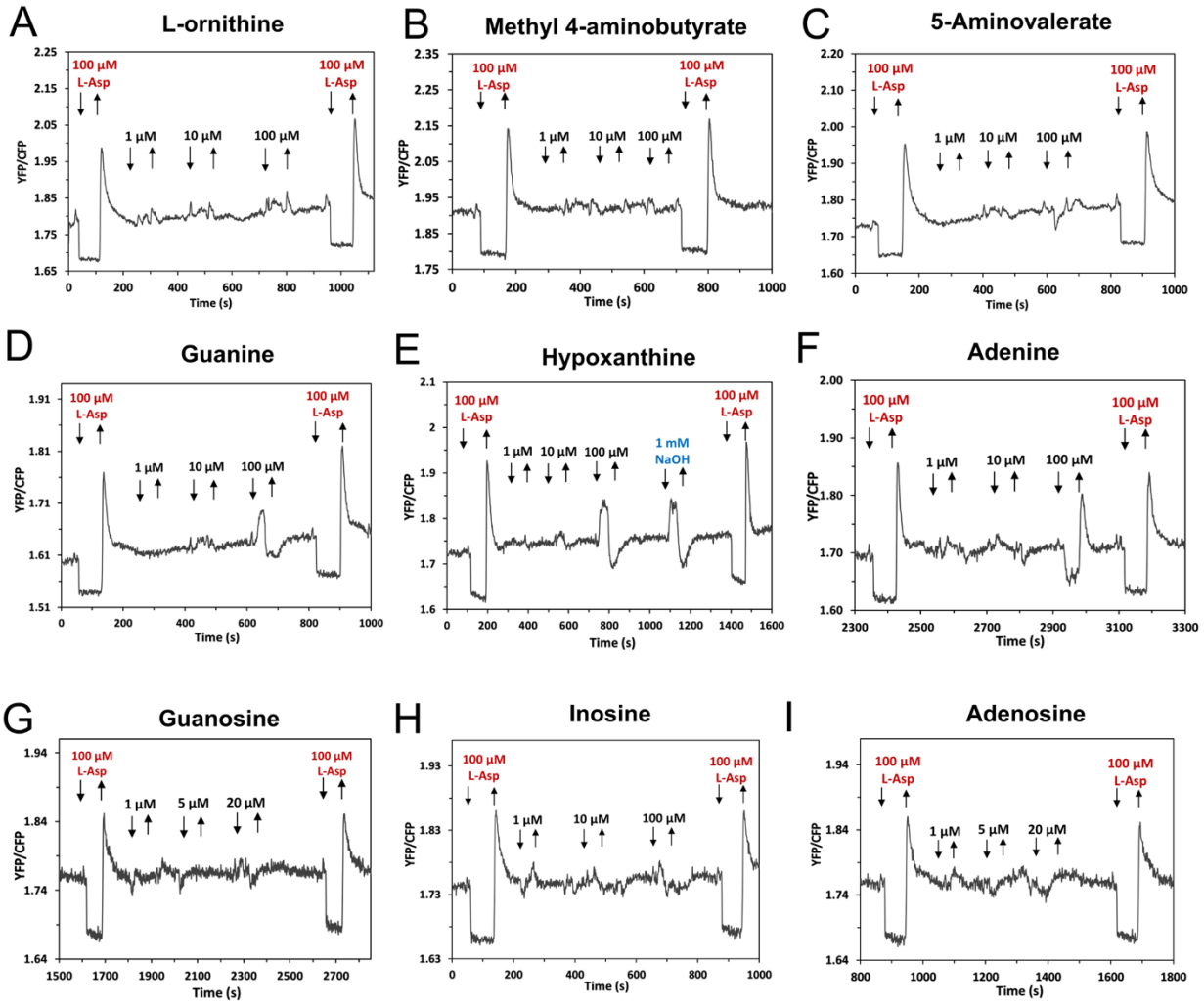

993

994 **Fig. S2 Responses of Tar control to different doses of characterized ligands.** FRET measurements of responses
995 in receptorless *E. coli* expressing Tar as a sole receptor to indicated concentrations of different compounds**.** 100 μM
996 L-aspartate (L-Asp) were used as positive ligand for Tar. Since guanine and hypoxanthine are only soluble at high
997 concentrations in alkalic solutions, an equivalent concentration of NaOH was used as negative control.

998

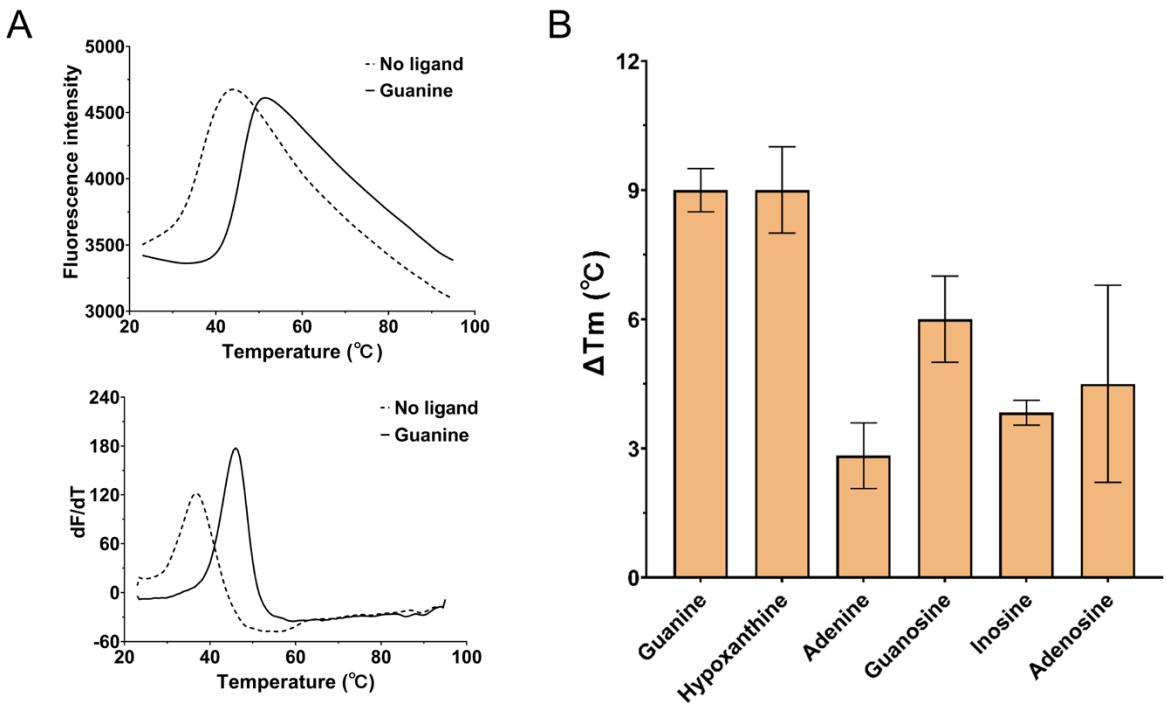

Fig. S3 Thermal stability of PctP-LBD is enhanced by purine derivatives. Thermal shift assay for purified PctP-LBD in presence of 2 mM guanine, hypoxanthine, adenine, guanosine, inosine or adenosine. (A) The thermal unfolding curves of PctP-LBD in the absence and presence of guanine; upper panel: raw data, lower panel: first derivative of raw data. (B) Increases in the midpoint of protein unfolding transition (Tm) induced by different ligands. Data shown are the means and standard deviations from three biological replicates conducted in triplicate.

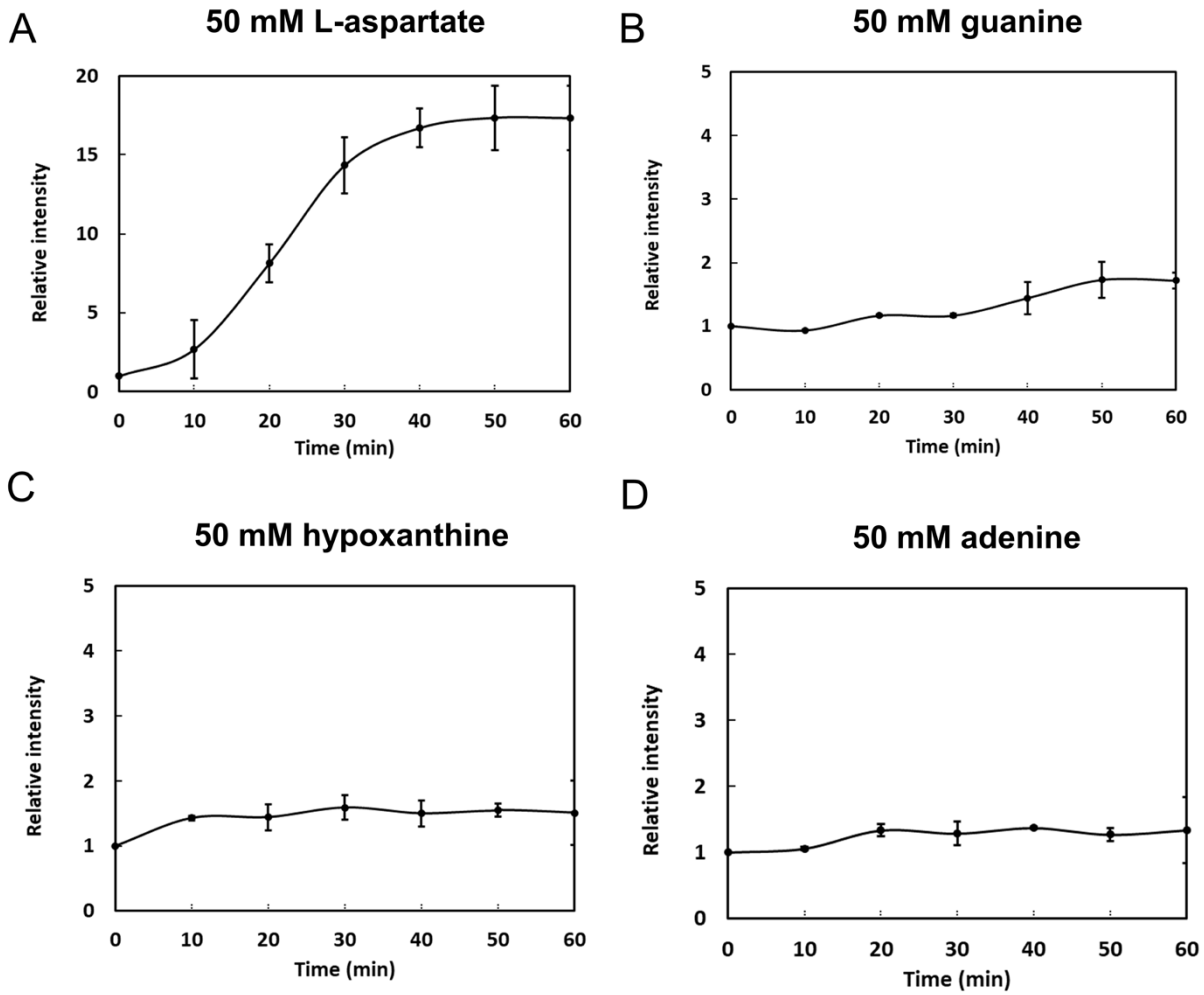

Fig. S4 Microfluidic assays of the chemotactic responses of *E. coli* expressing Tar as the sole receptor. Relative cell density (fluorescence intensity) in the observation channel over time in gradients of L-aspartate, guanine, hypoxanthine, and adenine with 50 mM in the source channel.

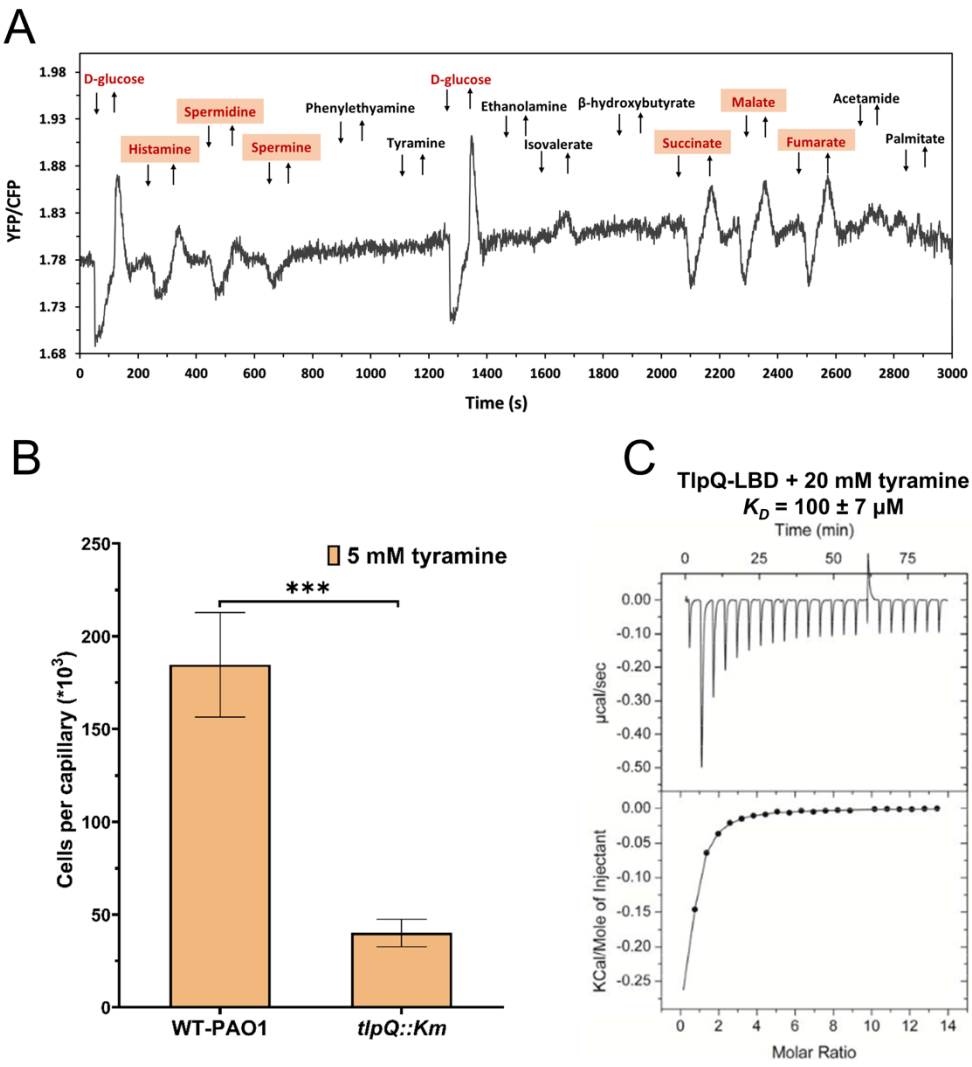

1013

1014 **Fig. S5 Characterization of TlpQ as a specific chemoreceptor for tyramine.** (A) Screening of unassigned
1015 potential ligands for TlpQ-Tar using FRET. FRET measurement was performed with receptorless *E. coli* cells
1016 expressing TlpQ-Tar as the sole receptor exposed to a stepwise addition (down arrow) and subsequent removal (up
1017 arrow) of 100 µM D-glucose (positive ligand for chimeras), three known ligands (histamine, spermine and
1018 spermidine) and other chemical compounds. The chemoattractants were shown in red. (B) Capillary chemotaxis
1019 assays of *tlpQ* deficient strain and WT-PAO1 (WT-Hiroshima) to 5 mM tyramine. Data are shown as the means and
1020 standard deviations from three biological replicates conducted in triplicate. (C) Microcalorimetric studies showing
1021 the binding of tyramine to TlpQ-LBD. The lower panels are the integrated, dilution heat corrected and concentration
1022 normalized peak areas fitted with the single-site binding model.

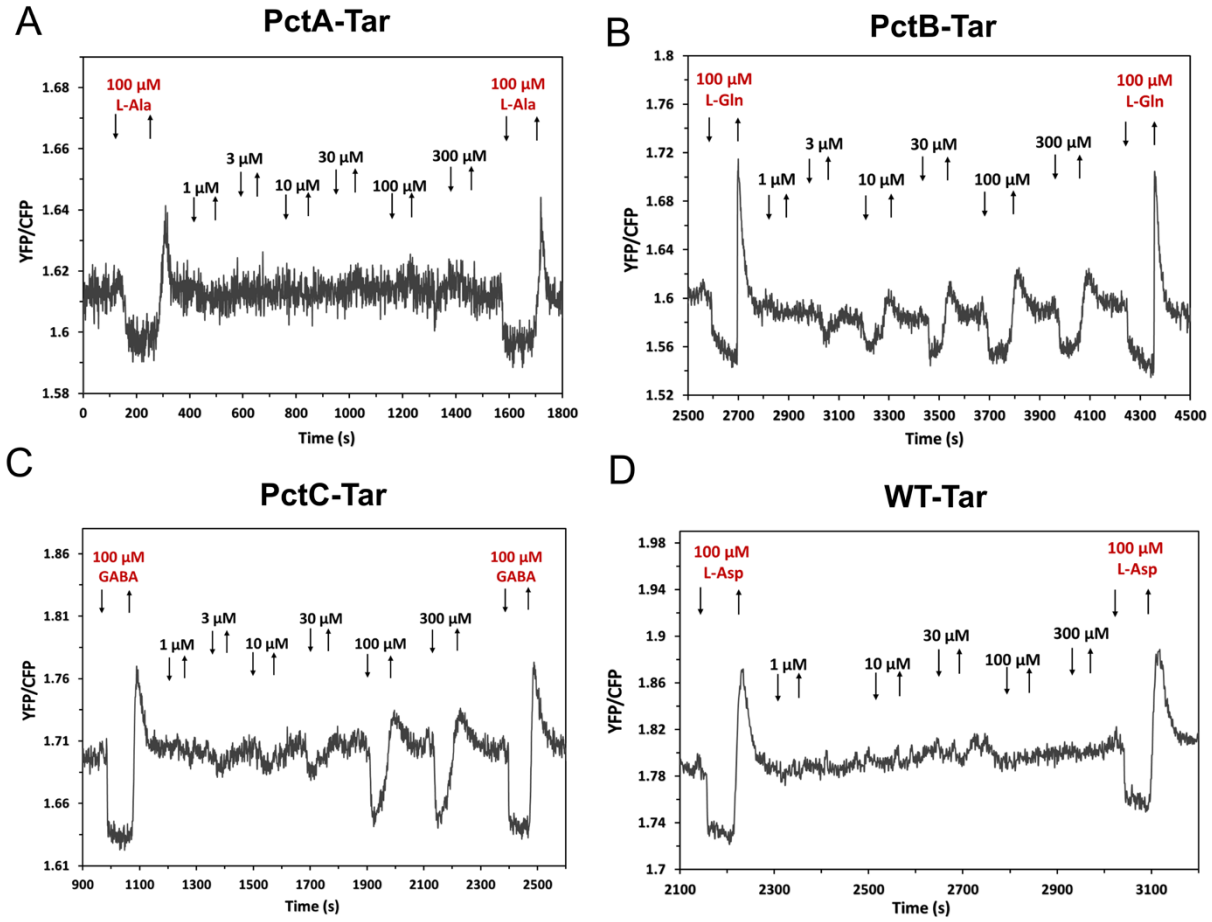

1023

1024 **Fig. S6 PctB and PctC mediate responses to histamine.** FRET measurements of responses mediated by PctA-Tar

1025 (A), PctB-Tar (B), PctC-Tar (C) or Tar (D) as a sole receptor to indicated concentrations of histamine. 100 μM L-

1026 aspartate (L-Asp) were used as positive control for Tar.

1027

1028

Table S1 Growth of *P. aeruginosa* PAO1 in M9 minimal medium supplemented with each of the compounds present in the Biolog plates PM1, PM2A and PM3B as nitrogen source (in nitrogen-free medium) or carbon source (in carbon-free medium). There are 202 that supported bacterial growth at different levels. Compounds were divided into different groups according to the magnitude of growth. The 39 highlighted compounds were further studied using quantitative capillary chemotaxis assays (Fig. 1).

Table S2 Summary of FRET responses of 16 hybrid chemoreceptors in the presence of 100 μM ligands. "A": attractant response; "R": repellent response; "*": strong response; "*R or A*": weak response (or unspecific response); "--": no response; "blank": no analysis. The yellow highlights were considered as positive ligands.

Table S3 Strains, plasmids and oligonucleotides used in this study.

Table S4. Experimental conditions used for microcalorimetric titrations.